Contents lists available at ScienceDirect

Physics Letters B

www.elsevier.com/locate/physletb

Evidence of rescattering effect in Pb–Pb collisions at the LHC through production of K*(892)^0 and ϕ(1020) mesons

ALICE Collaboration*

ABSTRACT

Measurements of K*(892)^0 and ϕ(1020) resonance production in Pb–Pb and pp collisions at $\sqrt{s_{NN}} = 5.02$ TeV with the ALICE detector at the Large Hadron Collider are reported. The resonances are measured at midrapidity ($|y| < 0.5$) via their hadronic decay channels and the transverse momentum (p_T) distributions are obtained for various collision centrality classes up to $p_T = 20$ GeV/c. The p_T-integrated yield ratio K*(892)^0/K in Pb–Pb collisions shows significant suppression relative to pp collisions and decreases towards more central collisions. In contrast, the ϕ(1020)/K ratio does not show any suppression. Furthermore, the measured K*(892)^0/K ratio in central Pb–Pb collisions is significantly suppressed with respect to the expectations based on a thermal model calculation, while the ϕ(1020)/K ratio agrees with the model prediction. These measurements are an experimental demonstration of rescattering of K*(892)^0 decay products in the hadronic phase of the collisions. The K*(892)^0/K yield ratios in Pb–Pb and pp collisions are used to estimate the time duration between chemical and kinetic freeze-out, which is found to be $\sim$ 4–7 fm/c for central collisions. The p_T-differential ratios of K*(892)^0/K, ϕ(1020)/K, K*(892)^0/π, ϕ(1020)/π, p/K*(892)^0 and p/ϕ(1020) are also presented for Pb–Pb and pp collisions at $\sqrt{s_{NN}} = 5.02$ TeV. These ratios show that the rescattering effect is predominantly a low-p_T phenomenon.

© 2020 The Author(s). Published by Elsevier B.V. This is an open access article under the CC BY license (http://creativecommons.org/licenses/by/4.0/). Funded by SCOAP^3.

1. Introduction

Several measurements in high-energy heavy-ion collisions at the Large Hadron Collider (LHC) [1–3] and the Relativistic Heavy Ion Collider (RHIC) [4–9] have shown that a strongly-coupled Quark-Gluon Plasma (QGP) is formed that subsequently hadronizes. Resonances, short lived hadrons that decay via strong interactions, play an important role in characterizing the properties of hadronic matter formed in heavy-ion collisions [10–16]. Several resonances have been observed in pp and nuclear collisions [10–19]: f_2(1270), ρ(770)^0, Δ(1232)$^{++}$, f_0(980), K*(892)$^{0,\pm}$, Σ(1385), Λ(1520) and ϕ(1020) with lifetimes of the order of 1.1 fm/c, 1.3 fm/c, 1.6 fm/c, 2.6 fm/c, 4.16 fm/c, 5.5 fm/c, 12.6 fm/c and 46.3 fm/c, respectively [20]. The wide range of their lifetimes allows them to be good probes of the dynamics of the system formed in ultra-relativistic heavy-ion collisions [21–27].

In the hadronic phase of the evolution of the system formed in heavy-ion collisions, there are two important temperatures and corresponding timescales: the chemical freeze-out, when the inelastic collisions among the constituents are expected to cease, and the later kinetic freeze-out, when all (elastic) interactions stop [28–30]. If resonances decay before kinetic freeze-out, then their decay products are subject to hadronic rescattering that alters their momentum distributions. This leads to inability to reconstruct the parent resonance using the invariant mass technique, resulting in a decrease in the measured yield relative to the primordial resonance yield, i.e. the yield at chemical freeze-out. The fraction of resonances that cannot be recovered depends on the lifetime of the hadronic phase (defined as the time between chemical and kinetic freeze-out), the hadronic interaction cross section of resonance decay products, the particle density in the medium and the resonance phase space distributions. For example, a pion from a K*(892)^0 meson decay could scatter with another pion in the medium as $\pi^-\pi^+ \to \rho^0 \to \pi^-\pi^+$. At the same time, after the chemical freeze-out, pseudoelastic interactions could regenerate resonances in the medium, leading to an enhancement of their yields. For example, interactions like $\pi K \to$ K*(892)$^0 \to \pi K$ and $K^-K^+ \to \phi$(1020) $\to K^-K^+$ could happen until kinetic freeze-out. Hence, resonances are probes of the rescattering and regeneration processes during the evolution of the fireball from chemical to kinetic freeze-out. Indeed, transport-based model calculations show that both rescattering and regeneration processes affect the final resonance yields [31,32]. Thermal statistical models, which have successfully explained a host of particle yields in heavy-ion collisions across a wide range of center-of-mass energies [33–36], are

able to explain the measured resonance yields only after including rescattering effects [37,38].

In this paper, the measurement of the production of K*(892)^0 and ϕ(1020) vector mesons at midrapidity in Pb–Pb and pp collisions at $\sqrt{s_{NN}}$ = 5.02 TeV is presented. Although both vector mesons have similar masses, their lifetime differs by a factor of larger than 10. This aspect is exploited to establish the dominance of rescattering in central Pb–Pb collisions at the LHC. The kaon and pion daughters of the short-lived K*(892)^0 → Kπ rescatter with other hadrons in the medium. The magnitude of the effect is mainly determined by the pion-pion interaction cross section [39], which is measured to be significantly larger (factor 5) than the total kaon-pion interaction cross section [40]. The latter determines the magnitude of the regeneration effect [41]. Thus with rescattering dominating over regeneration, the observable K*(892)^0 yields should decrease compared to the primordial yields, and therefore, a suppression of the K*(892)^0/K yield ratio is expected in heavy-ion collisions relative to pp collisions. Furthermore, this ratio is expected to decrease with increase in system size, which is determined by the collision centrality (maximum for central collisions). In contrast, because of a larger lifetime compared to that of the hadronic phase, the ϕ(1020) meson yields are not expected to be affected by rescattering [14,32]. The ϕ(1020) mesons are also expected not to be affected by the regeneration due to significantly lower KK cross section compared to Kπ and $\pi\pi$ cross sections [39,40]. Hence the independence of the ϕ(1020)/K yield ratio of the system size will act as a baseline for corresponding K*(892)^0/K measurements, thereby supporting the presence of the rescattering effect in heavy-ion collisions. The lower K*(892)^0/K yield ratio in Pb–Pb collisions compared to pp at the same $\sqrt{s_{NN}}$ can then be used to estimate the time span between chemical and kinetic freeze-out in heavy-ion collisions. Furthermore, due to the scattering of the decay products, the low-p_T K*(892)^0 are less likely to escape the hadronic medium before decaying, compared to high-p_T K*(892)^0 [32]. This could alter the K*(892)^0 p_T spectra in Pb–Pb collisions compared to pp, while no such effect is expected for ϕ mesons. Therefore, studying p_T-differential ratios of K*(892)^0 and ϕ(1020) mesons with respect to other non-strange (π) and strange (K) mesons, and baryons (p) in Pb–Pb and pp collisions will help to establish the p_T dependence of rescattering effects and disentangle them from other physics processes like radial flow that modifies the shapes of the p_T distributions at low and intermediate transverse momenta. In addition, the measurements at $\sqrt{s_{NN}}$ = 5.02 TeV are compared to results from Pb–Pb collisions at $\sqrt{s_{NN}}$ = 2.76 TeV [14,42]. Since production of particles and antiparticles is equal at midrapidity at LHC energies, the average of the yields of K*(892)^0 and $\overline{K}$*(892)^0 is presented in this paper and is denoted by the symbol K*^{0} unless specified otherwise. The ϕ(1020) is denoted by the symbol ϕ.

The paper is organized as follows: In section 2, the detectors used in the analysis are briefly described. In section 3, the dataset, the analysis techniques, the procedure for extraction of the yields of K*^{0} and ϕ mesons and the study of the systematic uncertainties are presented. In section 4, the yields obtained by invariant mass reconstruction of K*^{0} and ϕ mesons as a function of transverse momentum in Pb–Pb and pp collisions at $\sqrt{s_{NN}}$ = 5.02 TeV, the p_T-integrated ratios of K*^{0} and ϕ relative to charged kaons, and p_T-differential ratios relative to charged π, K and protons are reported. Finally, in section 5 the findings are summarized.

2. Experimental apparatus

The measurements of K*^{0} and ϕ meson production in pp and Pb–Pb collisions have been performed using the data collected by the ALICE detector in the year 2015. The details of the ALICE de-

tector can be found in Refs. [43–45]. So we briefly focus on the following main detectors used for this analysis. The forward V0 detector, a scintillator detector with a timing resolution less than 1 ns, is used for centrality selection, triggering and beam-induced background rejection. The V0 consists of two sub-detectors, V0A and V0C, placed at asymmetric positions, one on each side of the interaction point with full azimuthal acceptance and cover the pseudorapidity ranges 2.8 < η < 5.1 and -3.7 < η < -1.7, respectively. The centrality classes in Pb–Pb collisions are determined from the sum of the measured signal amplitudes in V0A and V0C, as discussed in Refs. [46,47]. The collision time information is provided by T0 which consist of two arrays of Cherenkov counters T0A and T0C, positioned on both sides of the interaction point [48]. The Zero Degree Calorimeter (ZDC) consists of two tungsten-quartz neutron and two brass-quartz proton calorimeter placed at a distance of 113 m on both sides of the interaction point. It is used to reject the background events and to measure the spectator nucleons.

In the central barrel, the Inner Tracking System (ITS) and the Time Projection Chamber (TPC) are used for charged-particle tracking and primary collision vertex reconstruction. The ITS consists of three sub-detectors of two layers each, covering a central pseudorapidity range |η| < 0.9: Silicon Pixel Detector (SPD), Silicon Drift Detector (SDD) and Silicon Strip Detector (SSD). The TPC is the main charged particle tracking detector, and has full azimuthal coverage in the pseudorapidity range |η| < 0.9. Along with track reconstruction, it also provides a measurement of the momentum and excellent particle identification (PID). The TPC provides the measured specific energy loss (dE/dx) to identify the particles, especially in low momentum range (p < 1 GeV/c) where the dE/dx of particles are well separated. To extend the particle identification to higher p_T, the Time of Flight (TOF) detector is used in addition to the TPC information. The TOF is based on the Multigap Resistive Plate Chamber (MRPC) technology and measures the arrival times of particles with a resolution of the order of 80 ps. It covers a pseudorapidity range |η| < 0.9 and provides excellent PID capabilities in the intermediate p_T range by exploiting the time-of-flight information.

3. Data sample and analysis details

The pp data were collected using a minimum bias (MB) trigger. The logic for MB trigger requires at least one hit in V0A or V0C and one hit in the central barrel detector SPD in coincidence with the LHC bunch crossing [49,50]. In pp collisions, a criterion based on the offline reconstruction of multiple primary vertices in the SPD [45] is applied to reduce the pileup, which is caused by multiple interactions in the same bunch crossing. The rejected pileup events are less than 1% of the total events. The Pb–Pb data were also collected using a MB trigger with a logic that requires a coincidence of signals in V0A and V0C. The MB-triggered events are analyzed if they have a reconstructed collision vertex whose position along the beam axis (V_z, z is the longitudinal direction) is within 10 cm from the nominal interaction point in both pp and Pb–Pb collisions. Background events are rejected using the timing information from the Zero Degree Calorimeters (ZDCs) and V0 detectors.

The Pb–Pb analysis is performed in 8 centrality classes defined in Ref. [46]: 0–10%, 10–20%, 20–30%, 30–40%, 40–50%, 50–60%, 60–70% and 70–80%. The 0–10% class corresponds to the most central Pb–Pb collisions, with small impact parameter, while the 70–80% class corresponds to peripheral Pb–Pb collisions, with large impact parameter. The total number of events that are analyzed after passing the event selection criteria are ∼110 million for pp and ∼30 million for Pb–Pb collisions. Charged tracks are selected

for analysis based on track selection criteria that ensure good track quality, as done in previous work [42]. In particular, a track in the TPC is requested to have a minimum of 70 crossed rows (horizontal segments along the transverse readout plane of the TPC) out of a maximum possible 159 [51]. A p_T-dependent selection criterion on the distance of closest approach to the collision vertex in the transverse (xy) plane (DCA_{xy}) and along the longitudinal direction (DCA_z) is used to reduce the contamination from secondary charged particles coming from weakly decaying hadrons. In addition to these selection criteria, tracks are required to have $p_T >$ 0.15 GeV/c in both pp and Pb–Pb collisions. Charged particles are accepted in the pseudorapidity range $|\eta| < 0.8$, which ensures a uniform acceptance.

The particle identification exploits both the TPC and the TOF. For K^{*0} and ϕ reconstruction in Pb–Pb collisions, charged particles are identified as pion or kaon if the mean specific energy loss ($\langle dE/dx \rangle$) measured by the TPC falls within two standard deviations ($2\sigma_{TPC}$) from the expected dE/dx values for π or K over the entire momentum range. If the TOF information is available for the track, in addition to the TPC, a TOF-based selection criterion $3\sigma_{TOF}$ is applied over the measured momentum range, where σ_{TOF} is the standard deviation from the expected time-of-flight for a given species. These requirements help in reducing the background under the signal peak over a large momentum range and provide a better separation between signal and background with respect to TPC PID only. For K^{*0} reconstruction in pp collisions, the same PID selection criteria are applied to identify pion and kaon candidates as are used in Pb–Pb collisions. For the ϕ reconstruction in pp collisions, the kaon candidates are identified using a $6\sigma_{TPC}$, $4\sigma_{TPC}$ and $2\sigma_{TPC}$ selection on the measured dE/dx distributions in the momentum ranges $p < 0.3$ GeV/c, $0.3 < p < 0.4$ GeV/c and $p > 0.4$ GeV/c, respectively. On top of this, the TOF-based selection criterion of $3\sigma_{TOF}$ is applied over the entire measured momentum range in pp collisions if the TOF information is available.

3.1. Yield extraction, corrections and normalization

The K^{*0} and ϕ resonances are reconstructed by calculating the invariant mass of their decay products through the hadronic decay channels K$^{*0}(\overline{\text{K}}^{*0}) \rightarrow$ K$^+\pi^-$(K$^-\pi^+$) (Branching Ratio, BR = 66.666 $\pm$ 0.006% [20]) and $\phi \rightarrow$ K$^+$K$^-$ (BR = 49.2 $\pm$ 0.5% [20]), respectively. Oppositely charged K and π (or K) from the same event are paired to reconstruct the invariant mass distributions of K$^{*0}(\phi)$. The Kπ and KK pairs are selected in the rapidity range $|y| < 0.5$ in both pp and Pb–Pb collisions. The invariant mass distribution exhibits a signal peak and a large combinatorial background resulting from the uncorrelated Kπ (KK) pairs. The combinatorial background is estimated using a mixed-event technique in both collision systems. The mixed-event background is constructed by combining kaons from one event with the oppositely charged π(K) from different events for K$^{*0}(\phi)$. The events which are mixed are required to have similar characteristics. In Pb–Pb, two events are mixed if they belong to the same centrality class and the difference between the collision vertex position is $|\Delta V_z| < 1$ cm. In pp collisions, two events are mixed with a condition of $|\Delta V_z| <$ 1 cm and a difference in charged-particle density at midrapidity ($|\Delta y| < 0.5$) of less than 5. To minimize the statistical fluctuations in the background distribution, each event is mixed with five other ones. The invariant mass distribution from the mixed-event is normalized to the same-event oppositely-charged pair distribution in the mass region 1.1–1.3 (resp. 1.04–1.06) GeV/c^2 for K^{*0} (resp. ϕ), which is away from the mass peak (6Γ for K^{*0} and 7Γ for ϕ, Γ is the width of the resonance). After the combinatorial background subtraction, the signal peak is observed on top of a residual background. The latter is due to the correlated Kπ or KK

pairs that originate from jets and from the misidentification of particles. It is shown in Ref. [42] that the residual background has a smooth dependence on mass and the shape of the background is well described by a second order polynomial [14,42]. The invariant mass distributions after mixed-event background subtraction are fitted with a Breit-Wigner (resp. Voigtian) function for the signal peak of K^{*0} (resp. ϕ) plus a second order polynomial for the residual background [42]. The Voigtian function is a convolution of a Breit-Wigner distribution and a Gaussian, where the width σ of the Gaussian accounts for the mass resolution. The latter is p_T-dependent and varies between 1 and 2 MeV/c^2. The raw yields are measured as a function of p_T for K^{*0} and ϕ in pp collisions and in various centrality classes in Pb–Pb collisions. A detailed description of the yield extraction procedure is given in Ref. [42].

The measured yields are affected by the detector acceptance and reconstruction efficiency ($A \times \varepsilon_{rec}$). This is estimated by means of dedicated Monte Carlo simulations using the PYTHIA (PYTHIA 6 Perugia 2011 tune and PYTHIA 8 Monash 2013 tune) [52,53] and HIJING [54] event generators for pp and Pb–Pb collisions, respectively. The generated particles are then propagated through the detector material using GEANT3 [55]. The $A \times \varepsilon_{rec}$ is calculated as a function of p_T and is defined as the ratio of the reconstructed K$^{*0}(\phi)$ to the generated K$^{*0}(\phi)$, both within $|y| < 0.5$. For the reconstruction of resonances, the same track and PID selection criteria are applied to the simulations as used in the analysis of the measured data. The $A \times \varepsilon_{rec}$ is calculated for K$^{*0}(\phi)$ that decay through the hadronic channel K$^{\pm}\pi^{\mp}$ (K$^+$K$^-$), hence it does not include the correction for BR. In Pb–Pb collisions, the $A \times \varepsilon_{rec}$ has a weak centrality dependence and the raw yields are corrected using the $A \times \varepsilon_{rec}$ of the respective centrality class.

The procedure to correct the raw yields is given by

$$\frac{1}{N_{event}} \frac{d^2N}{dydp_T} = \frac{1}{N_{event}^{acc}} \frac{d^2N^{raw}}{dydp_T} \frac{\varepsilon_{trig} \cdot \varepsilon_{vert} \cdot \varepsilon_{sig}}{(A \times \varepsilon_{rec}) \cdot BR}. \tag{1}$$

The raw yields are normalized to the number of accepted events (N_{event}^{acc}) and corrected for $A \times \varepsilon_{rec}$, trigger efficiency ($\varepsilon_{trig}$), vertex reconstruction efficiency (ε_{vert}), signal loss (ε_{sig}) and the BR of the decay channel. The yields in pp are normalized to the number of inelastic collisions with a trigger efficiency correction, $\varepsilon_{trig} = 0.757$ $\pm$ 0.019 [56]. The vertex reconstruction efficiency in pp collisions is found to be $\varepsilon_{vert} = 0.958$. The signal loss correction factor ε_{sig} is determined based on MC simulations as a function of p_T and accounts for the resonance signal lost due to trigger inefficiencies. The $\varepsilon_{sig}(p_T)$ correction is only significant for $p_T < 2.5$ GeV/c and has a value of less than 5% both for K^{*0} and ϕ in pp collisions. In Pb–Pb collisions, the yields of K^{*0} and ϕ in a given centrality class are normalized by the number of events in the respective V0M (sum of V0A and V0C amplitude) event centrality class. The correction factors ε_{trig}, ε_{vert} and $\varepsilon_{sig}(p_T)$ are compatible with unity in the reported centrality classes in Pb–Pb collisions and hence are not used.
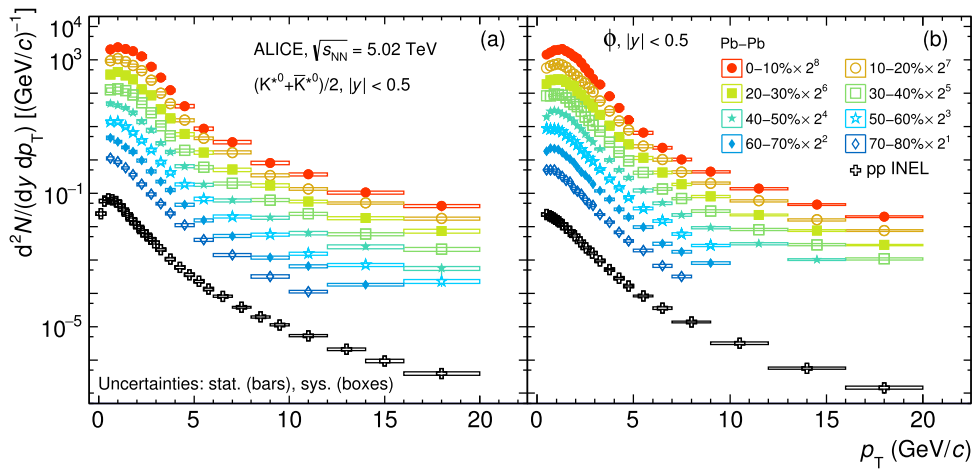
3.2. Systematic uncertainties

The systematic uncertainties in the measurement of K^{*0} and ϕ yields in pp and Pb–Pb collisions are summarized in Table 1. The sources of systematic uncertainties are related to the yield extraction method, PID and track selection criteria, global tracking efficiency, the knowledge of the ALICE material budget and of the interaction cross section of hadrons in the detector material. The uncertainties are reported for three transverse momentum values, low, mid and high p_T. For Pb–Pb collisions all the systematic uncertainties except the one related to the yield extraction are common in the various centrality classes and the values given in the

Table 1

Systematic uncertainties in the measurement of K^{*0} and ϕ yields in pp and Pb–Pb collisions at $\sqrt{s_{NN}} = 5.02$ TeV. These uncertainties are shown for three transverse momentum values, low, mid and high p_T. For Pb–Pb collisions all the systematic uncertainties except yield extraction are common in various centrality classes and the values given in the table are averaged over all centrality classes.

Systematic variation	Pb–Pb						pp					
	K^{*0}			ϕ			K^{*0}			ϕ		
	p_T (GeV/c)			p_T (GeV/c)			p_T (GeV/c)			p_T (GeV/c)		
	0.6	4.5	18	0.5	4.25	18	0.1	4.25	18	0.5	4.25	18
Yield extraction (%)	7.3	7.5	10.1	4.4	1.9	4.9	11.8	7.9	8.2	2.4	3.5	3.5
Track selection (%)	2.7	1.4	3.0	3.0	1.3	1.0	1.4	1.0	1.9	4.0	2.0	5.5
Particle identification (%)	5.4	3.0	5.0	1.0	1.5	2.4	2.1	3.2	6.9	0.3	1.7	6.5
Global tracking efficiency (%)	4.7	7.4	4.0	4.7	8.2	3.1	2.0	3.1	3.4	2.0	3.2	2.4
Material budget (%)	1.4	0	0	5.7	0	0	3.4	0	0	5.7	0	0
Hadronic Interaction (%)	2.4	0	0	1.3	0	0	2.8	0	0	1.3	0	0
Total (%)	10.9	11.0	12.3	9.2	8.6	6.4	13.0	9.1	11.4	7.7	5.4	9.5

Fig. 1. The p_T distributions of (a) K^{*0} and (b) ϕ mesons in pp collisions and various centrality classes in Pb–Pb collisions at $\sqrt{s_{NN}} = 5.02$ TeV. The values are plotted at the center of each bin. The statistical and systematic uncertainties are shown as bars and boxes, respectively.

table are averaged over all centralities. The yield extraction method includes the uncertainties due to variations of the fitting range, the choice of combinatorial background estimation technique, normalization range and residual background shape. The uncertainties due to yield extraction are estimated to be 7.9–11.8% for K^{*0} (resp. 2.4–3.5% for the ϕ) in pp and 7.3–10.1% (resp. 1.9–4.9%) in Pb–Pb collisions. The PID systematic uncertainties varies between 2.1–6.9% (0.3–6.5%) for K^{*0} (ϕ) in pp and Pb–Pb collisions. The contribution to the uncertainty from the global tracking efficiency is calculated from the corresponding values for single charged particles [51] and results in a 2.0–8.2% uncertainty by combining the two charged tracks used in the invariant mass reconstruction of K^{*0} and ϕ. The contribution from variation of the track selection criteria is 1.0–5.5%. The systematic uncertainties due to the hadronic interaction cross section are estimated to be less than 2.8% and contribute only at low p_T (< 2 GeV/c). The uncertainties in the description of the material budget of ALICE detector subsystems in GEANT3 (see Ref. [57] for details) give a contribution lower than 5.7% on the yields of K^{*0} and ϕ in pp and Pb–Pb collisions. The material budget uncertainty is significant only at p_T < 2 GeV/c and negligible at higher p_T. The total p_T-dependent systematic uncertainties on the $K^{*0}(\phi)$ yields are estimated to be 9.1–13.0% (5.4–9.5%) in pp collisions and 10.9–12.3% (6.4–9.2%) in Pb–Pb collisions. The common systematic uncertainties for different particles (global tracking efficiency, material budget and

hadronic interaction) are canceled out in calculating particle yield ratios like K^{*0}/K and ϕ/K.

4. Results and discussion

4.1. Transverse momentum spectra in pp and Pb–Pb collisions

The p_T distributions of the K^{*0} and ϕ mesons for $|y| < 0.5$, normalized to the number of events and corrected for efficiency, acceptance and branching ratio of the decay channel, are shown in Fig. 1. The results for Pb–Pb collisions are presented for eight different centrality classes (0–10% up to 70–80% in 10% wide centrality intervals) together with the results from inelastic pp collisions at the same energy.

The p_T-integrated particle yields have been extracted using the procedure described in Refs. [14,42]. The p_T distributions are fitted with a Lévy-Tsallis function [58,59] in pp and a Boltzmann-Gibbs blast-wave function [60] in Pb–Pb collisions. The yields have been extracted from the data in the measured p_T region and the fit functions have been used to extrapolate into the unmeasured (low and high p_T) region. The low-p_T extrapolation covers $p_T < 0.4$ GeV/c for $K^{*0}(\phi)$ and accounts for 8.6% (7.2%) and 12.5% (12.7%) of the total yield in the 0–10% and 70–80% centrality classes in Pb–Pb collisions, respectively. In pp collisions, the K^{*0} is measured in the range $0 < p_T < 20$ GeV/c. For the ϕ meson, the low-p_T extrapolation covers $p_T < 0.4$ GeV/c, accounting for 15.7% of the total
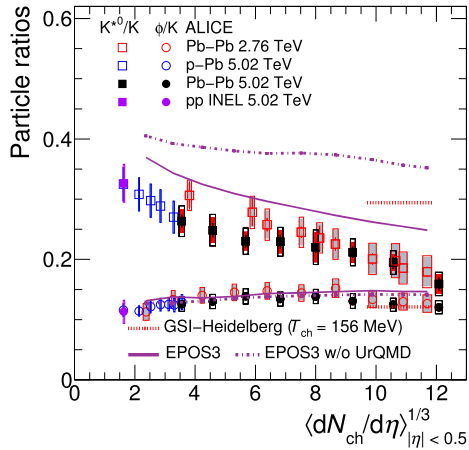
Fig. 2. p_T-integrated particle yield ratios K^{*0}/K$^-$ and ϕ/K$^-$ as a function of $\langle dN_{ch}/d\eta\rangle^{1/3}$ measured at midrapidity in pp, p–Pb and Pb–Pb collisions at $\sqrt{s_{NN}}$ = 5.02 TeV. For Pb–Pb collisions at $\sqrt{s_{NN}}$ = 2.76 TeV, the ϕ/K$^-$ values are taken from Ref. [14] and the K^{*0}/K$^-$ values are taken from Ref. [42]. The ratios for p–Pb collisions are taken from Ref. [17]. Statistical uncertainties (bars) are shown together with total (hollow boxes) and charged-particle multiplicity-uncorrelated (shaded boxes) systematic uncertainties. Thermal model calculations with chemical freeze-out temperature T_{ch} = 156 MeV for the most central Pb–Pb collisions [34,64] are also shown. EPOS3 model predictions [32] of K^{*0}/K and ϕ/K ratios in Pb–Pb collisions are also shown as violet lines.

yield. The extrapolated fraction of the yield is negligible for $p_T >$ 20 GeV/c.

4.2. Particle ratios

Fig. 2 shows the K^{*0}/K and ϕ/K ratios as a function of $\langle dN_{ch}/d\eta\rangle^{1/3}$ [46,47,51] for Pb–Pb collisions at $\sqrt{s_{NN}}$ = 2.76 [14, 42] and 5.02 TeV, p–Pb collisions at $\sqrt{s_{NN}}$ = 5.02 TeV [17] and pp collisions at $\sqrt{s}$ = 5.02 TeV. The kaon yields in Pb–Pb at $\sqrt{s_{NN}}$ = 5.02 TeV are from Ref. [51]. The $\langle dN_{ch}/d\eta\rangle^{1/3}$ measured at midrapidity, is used here as a proxy for the system size. This is supported by the observation of the linear increase in the HBT radii with $\langle dN_{ch}/d\eta\rangle^{1/3}$ [61,62]. The K^{*0}/K ratio decreases for rising $\langle dN_{ch}/d\eta\rangle^{1/3}$ while the ϕ/K ratio is almost independent of $\langle dN_{ch}/d\eta\rangle^{1/3}$. The ratios exhibit a smooth trend across the different collision systems and collision energies studied. The K^{*0}/K and ϕ/K ratios in Pb–Pb collisions at $\sqrt{s_{NN}}$ = 2.76 and 5.02 TeV are in agreement within uncertainties.

The resonance yields are modified during the hadronic phase by rescattering (which would reduce the measured yields) and regeneration (which would increase the measured yields). The observed dependence of the K^{*0}/K ratio on the charged-particle multiplicity is consistent with the behavior that would be expected if rescattering is the cause of the suppression. The fact that the ϕ/K ratio does not exhibit suppression with charged-particle multiplicity suggests that the ϕ, which has a lifetime an order of magnitude larger than that of the K^{*0}, decays predominantly outside the hadronic medium. Theoretical estimates suggest that about 55% of the of K^{*0} mesons with momentum p = 1 GeV/c, decay within 5 fm/c of production (a typical estimate for the time between chemical and kinetic freeze-out in heavy-ion collisions [22,32,63]), while only 7% of ϕ mesons with p = 1 GeV/c decay within that time. This supports the hypothesis that the experimentally observed decrease of the K^{*0}/K ratio with charged-particle multiplicity is caused by rescattering. A similar suppression has also been observed for ρ^0/π [15] and Λ^*/Λ [13] in central Pb–Pb collisions relative to peripheral Pb–Pb and pp collisions at $\sqrt{s_{NN}}$ = 2.76 TeV. In addition, the K^{*0}/K ratio from thermal model calculations without rescattering effects and with chemical freeze-out temperature
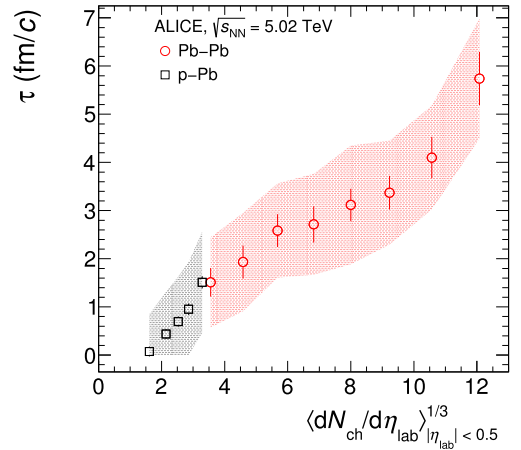
Fig. 3. Lower limit on the hadronic phase lifetime between chemical and kinetic freeze-out as a function of $\langle dN_{ch}/d\eta\rangle^{1/3}$ in p–Pb [17] and Pb–Pb collisions at $\sqrt{s_{NN}}$ = 5.02 TeV. The bars and bands represent the statistical and systematic uncertainties, respectively, propagated to the lifetime from the uncertainties associated with the measured K^{*0}/K ratios in Pb–Pb (p–Pb) and pp collisions at $\sqrt{s_{NN}}$ = 5.02 TeV.

T_{ch} = 156 MeV for the most central Pb–Pb collisions [34,64] is found to be higher than the corresponding measurements, while the measured ϕ/K ratio agrees with the thermal model predictions. The K^{*0}/K and ϕ/K ratios in Pb–Pb collisions are also compared to EPOS3 model calculations with and without a hadronic cascade phase modeled by UrQMD [32]. The EPOS3 model predictions shown in the figure are for Pb–Pb collisions at $\sqrt{s_{NN}}$ = 2.76 TeV but no significant qualitative differences are expected between the two energies. The EPOS3 generator with UrQMD reproduces the observed trend of the K^{*0}/K and ϕ/K ratios which further supports the experimental data.

The fact that K^{*0}/K$^-$ decreases with increasing $\langle dN_{ch}/d\eta\rangle^{1/3}$ implies that rescattering of the decay products of K^{*0} in the hadronic phase is dominant over K^{*0} regeneration. This suggests that K^{*0} $\leftrightarrow$ Kπ is not in balance. Hence in Pb–Pb the K^{*0}/K$^-$ ratio can be used to get an estimate of the time between chemical and kinetic freeze-out, τ, as, [K^{*0}/K$^-$]$_{kinetic}$ = [K^{*0}/K$^-$]$_{chemical}$ $\times$ $e^{-\tau/\tau_{K^{*0}}}$, where $\tau_{K^{*0}}$ is the K^{*0} lifetime. Here, $\tau_{K^{*0}}$ is taken as 4.16 fm/c ignoring any medium modification of the width of the invariant mass distribution of K^{*0}. Furthermore, it is assumed that [K^{*0}/K$^-$]$_{chemical}$ is given by the values measured in pp collisions and the Pb–Pb collision data provides an estimate for [K^{*0}/K$^-$]$_{kinetic}$. This is equivalent to assuming that all K^{*0}'s that decay before kinetic freeze-out are lost due to rescattering effects and there is no regeneration effect between kinetic and chemical freeze-out which is supported by AMPT simulations [31]. All the assumptions listed above lead to an estimate of τ as a lower limit for the time span between chemical and kinetic freeze-outs. A decrease in the K^{*0}/K ratio with increasing multiplicity has previously also been observed in p–Pb collisions at $\sqrt{s_{NN}}$ = 5.02 TeV [17]. This might indicate the presence of rescattering effect in high multiplicity p–Pb collisions and is suggestive of a finite lifetime of the hadronic phase. For comparison we have also estimated the hadronic phase lifetime in p–Pb data. Fig. 3 shows the results for τ boosted by a Lorentz factor ($\sim$ 1.65 for p–Pb collisions and 1.75 for Pb–Pb collision) as a function of $\langle dN_{ch}/d\eta\rangle^{1/3}$. Neglecting higher order terms, the Lorentz factor is estimated as $\sqrt{1 + (\langle p_T\rangle/mc)^2}$. Here m is the rest mass of the resonance and $\langle p_T\rangle$ is used as an approximation for p for the measurements at midrapidity. The time interval between chemical and kinetic freeze-out increases with the system size as expected. For central Pb–Pb collisions at $\sqrt{s_{NN}}$ = 5.02 TeV, the lower limit of time between chemical and
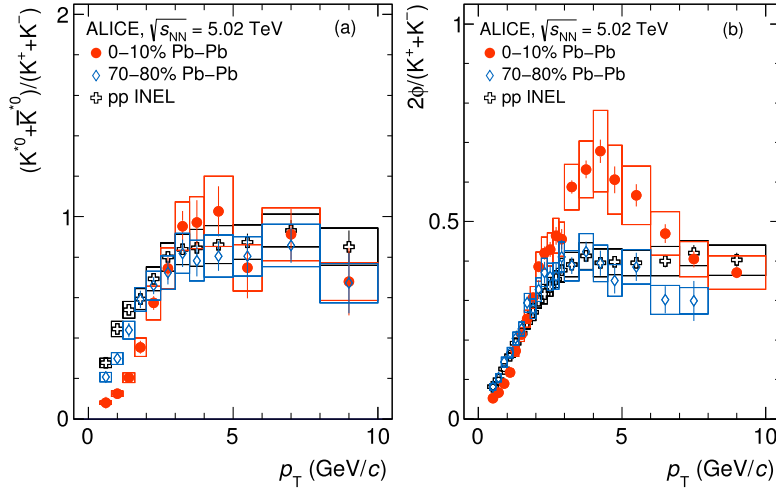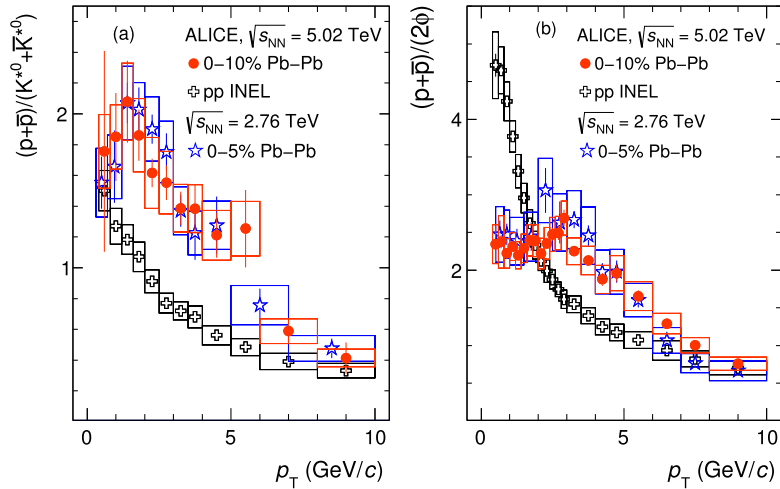
Fig. 4. Particle yield ratios $(K^{*0} + \overline{K}^{*0})/(K^+ + K^-)$ in panel (a) and $(2\phi)/(K^+ + K^-)$ in panel (b), both as a function of p_T for centrality classes 0–10% and 70–80% in Pb–Pb collisions at $\sqrt{s_{NN}} = 5.02$ TeV. For comparison, the corresponding ratios are also shown for inelastic pp collisions at $\sqrt{s} = 5.02$ TeV. The statistical uncertainties are shown as bars and systematic uncertainties are shown as boxes. In the text $(K^{*0} + \overline{K}^{*0})$, $(K^+ + K^-)$ are denoted by K^{*0} and K, respectively.
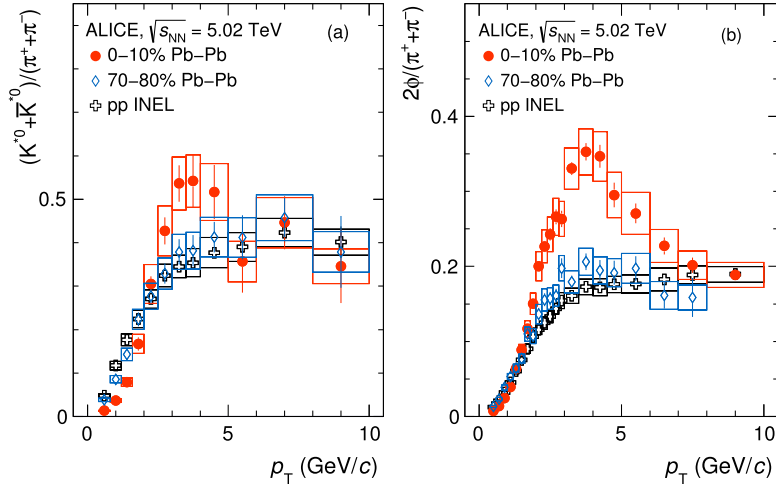
Fig. 5. Particle yield ratios $(K^{*0} + \overline{K}^{*0})/(\pi^+ + \pi^-)$ in panel (a) and $(2\phi)/(\pi^+ + \pi^-)$ in panel (b), both as a function of p_T for centrality classes 0–10% and 70–80% in Pb–Pb collisions at $\sqrt{s_{NN}} = 5.02$ TeV. For comparison, the corresponding ratios are also shown for inelastic pp collisions at $\sqrt{s} = 5.02$ TeV. The statistical uncertainties are shown as bars and systematic uncertainties are shown as boxes. In the text $(K^{*0} + \overline{K}^{*0})$, $(\pi^+ + \pi^-)$ are denoted by K^{*0} and π, respectively.

kinetic freeze-out is about 4–7 fm/c. This is of the same order of magnitude as the K^{*0} lifetime, but about an order of magnitude shorter than the ϕ lifetime. A smooth increase of τ with system size from p–Pb to Pb–Pb collisions is observed. The EPOS3 generator with UrQMD reproduces the increasing trend of τ with multiplicity qualitatively [32]. If a constant chemical freeze-out temperature is assumed, then the increase of τ with multiplicity in Pb–Pb collisions corresponds to a decrease of the kinetic freeze-out temperature. This is in qualitative agreement with results from blast-wave fits to identified particle p_T distributions [51], which are interpreted as decrease in the kinetic freeze-out temperature from peripheral to central collisions.

Further, to quantify the p_T-dependence of the rescattering effect observed in Pb–Pb collisions, a set of p_T-differential yield ratios was studied: K^{*0}/K, ϕ/K, K^{*0}/π, ϕ/π, p/K^{*0} and p/ϕ as shown in Figs. 4, 5 and 6. The choice of the ratios is motivated by the following reasons: (a) the ratio of resonance yields relative to the ones of kaons and pions can shed light on the shapes of the p_T distributions of mesons with different mass and quark content, and (b) the ratios of the proton yield with respect to the yields of the

resonances allow comparisons among hadrons of similar mass, but different baryon number and quark content to be made. For case (a), ratios in 0–10%, 70–80% Pb–Pb collisions and pp collisions at $\sqrt{s_{NN}} = 5.02$ TeV are compared. For case (b), ratios in 0–10% Pb–Pb collisions and pp collisions at $\sqrt{s_{NN}} = 5.02$ TeV are compared with 0–5% in Pb–Pb collisions at $\sqrt{s_{NN}} = 2.76$ TeV. The ratios for 70–80% in Pb–Pb collisions are closer to the corresponding results in pp collisions. Noticeably, there are distinct differences between central and peripheral (pp) collisions in the ratios for p_T below $\sim$ 2 GeV/c and intermediate p_T (between 2 and 6 GeV/c) but the ratios are consistent at higher p_T [42].

At low p_T, the K^{*0}/K and K^{*0}/π for central collisions are lower than in peripheral (pp) collisions, while the corresponding yield ratios for ϕ meson are comparable within the uncertainties. This observation is consistent with the suppression of K^{*0} yields due to rescattering in the hadronic phase. It demonstrates that rescattering affects low momentum particles. At intermediate p_T, both ratios show an enhancement for central Pb–Pb collisions relative to peripheral and pp collisions, which is more prominent for ϕ/K, ϕ/π and K^{*0}/π. This is consistent with the presence of a larger

Fig. 6. Particle yield ratios $(p + \overline{p})/(K^{*0} + \overline{K}^{*0})$ in panel (a) and $(p + \overline{p})/(2\phi)$ in panel (b), both as a function of p_T for 0–10% central Pb–Pb collisions and inelastic pp collisions at $\sqrt{s_{NN}} = 5.02$ TeV. For comparison, similar ratios are also shown for 0–5% central Pb–Pb collisions at $\sqrt{s_{NN}} = 2.76$ TeV [42]. The statistical uncertainties are shown as bars and systematic uncertainties are shown as boxes. In the text $(K^{*0} + \overline{K}^{*0})$ and $(p + \overline{p})$ are denoted by K^{*0} and p, respectively.

radial flow in central collisions relative to peripheral and pp collisions [51]. Given that the masses of K^{*0} and ϕ mesons are larger than those of the charged kaon and pion, the resonances experience a larger radial flow effect. In central Pb–Pb collisions, for p_T below 5 GeV/c, the p/ϕ ratio is observed to be independent of p_T and the p/K^{*0} ratio exhibits a weak p_T-dependence within the uncertainties, in contrast to the decrease of both ratios with p_T observed in pp collisions. In turn, this suggests that the shapes of the p_T distributions are similar for K^{*0}, ϕ and p in this p_T range. Although the quark contents are different, the masses of these hadrons are similar, indicating that this is the relevant quantity in determining spectra shapes. This is consistent with expectations from hydrodynamic-based models [65,66]. Within the uncertainties, the p/K^{*0} and p/ϕ ratios for central Pb–Pb collisions at $\sqrt{s_{NN}}$ = 5.02 TeV and 2.76 TeV [42] are constant at intermediate p_T. This is consistent with the observation of similar order radial flow at both energies, obtained from the analysis of p_T spectra of pions, kaons and protons [51]. For $p_T > 6$ GeV/c, the K^{*0}/K, ϕ/K, K^{*0}/π, ϕ/π, p/K^{*0} and p/ϕ yield ratios in central collisions are similar to peripheral and pp collisions, indicating that fragmentation is the dominant hadron production mechanism in this p_T region. This is consistent with previous measurements at $\sqrt{s_{NN}}$ = 2.76 TeV [42].

5. Summary

The transverse momentum distributions of K^{*0} and ϕ mesons have been measured at midrapidity ($|y| < 0.5$) for various collision centralities in Pb–Pb and inelastic pp collisions at $\sqrt{s_{NN}} = 5.02$ TeV using the ALICE detector. The K^{*0} yields relative to charged kaons in Pb–Pb collisions show a suppression with respect to pp collisions, which increases with the system size, quantified using $\langle dN_{ch}/d\eta \rangle^{1/3}$ measured at midrapidity. In contrast, no such suppression is observed for the ϕ mesons. The lack of suppression for the ϕ meson can be attributed to the fact that most of them decay outside the fireball because of its longer lifetime (τ_ϕ = 46.3 $\pm$ 0.4 fm/c). Because of a shorter lifetime ($\tau_{K^{*0}}$ = 4.16 $\pm$ 0.05 fm/c), a significant number of produced K^{*0} decays in the hadronic medium. The decay product(s) undergo interactions with other hadrons in the medium resulting in a significant change in their momentum, and no longer contributing to the K^{*0} signal reconstructed in the experiment. Although both rescattering and regeneration are possible, the results presented here represent an experimental demonstration of the predominance of rescattering effects in the hadronic phase of the system produced in heavy-ion collisions. The effect of rescattering increases with the system size. Furthermore, the K^{*0}/K yield ratios in central Pb–Pb collisions are significantly lower compared to the values from thermal model calculations without rescattering effects, while the measured ϕ/K yield ratio agrees with the model calculation. This further corroborates the hypothesis that rescattering affects the measured K^{*0} yields in Pb–Pb collisions. A lower limit for the lifetime of the hadronic phase is determined by using the K^{*0}/K ratios in Pb–Pb and pp collisions at $\sqrt{s_{NN}} = 5.02$ TeV. The lifetime, as expected, increases with system size. For central Pb–Pb collisions, it is about 4–7 fm/c.

The p_T-differential yield ratios of K^{*0}/π and K^{*0}/K are studied in central Pb–Pb, peripheral Pb–Pb and pp collisions to understand the p_T-dependence of the rescattering effect. It is observed that rescattering dominantly affects the hadrons at $p_T < 2$ GeV/c. At intermediate p_T (2–6 GeV/c), the ϕ/K, ϕ/π, K^{*0}/π, p/K^{*0} and p/ϕ yield ratios are enhanced in central Pb–Pb collisions relative to peripheral Pb–Pb and pp collisions. In addition, the spectral shapes of K^{*0}, ϕ and p, which have comparable masses, are similar within the uncertainties for p_T below 5 GeV/c in Pb–Pb collisions. These measurements demonstrate the effect of higher radial flow in central Pb–Pb collisions relative to peripheral Pb–Pb and pp collisions. A comparison of the p/K^{*0} and p/ϕ ratios for central Pb–Pb collisions at $\sqrt{s_{NN}} = 5.02$ and 2.76 TeV shows the constancy of the ratios with p_T. This is consistent with the observation of comparable radial flow at $\sqrt{s_{NN}} = 5.02$ TeV and 2.76 TeV. For higher p_T, above 6 GeV/c, all the ratios agree within the uncertainties for central and peripheral Pb–Pb, and pp collisions, indicating that particle production via fragmentation at high transverse momenta is not significantly modified in the presence of a medium.

Acknowledgements

References

[1] ALICE Collaboration, K. Aamodt, et al., Elliptic flow of charged particles in Pb–Pb collisions at 2.76 TeV, Phys. Rev. Lett. 105 (2010) 252302, arXiv:1011.3914 [nucl-ex].

[2] ALICE Collaboration, K. Aamodt, et al., Suppression of charged particle production at large transverse momentum in central Pb–Pb collisions at $\sqrt{s_{NN}} = 2.76$ TeV, Phys. Lett. B 696 (2011) 30–39, arXiv:1012.1004 [nucl-ex].

[3] ALICE Collaboration, K. Aamodt, et al., Higher harmonic anisotropic flow measurements of charged particles in Pb–Pb collisions at $\sqrt{s_{NN}}$=2.76 TeV, Phys. Rev. Lett. 107 (2011) 032301, arXiv:1105.3865 [nucl-ex].

[4] STAR Collaboration, J. Adams, et al., Experimental and theoretical challenges in the search for the quark gluon plasma: the STAR Collaboration's critical assessment of the evidence from RHIC collisions, Nucl. Phys. A 757 (2005) 102–183, arXiv:nucl-ex/0501009 [nucl-ex].

[5] PHENIX Collaboration, K. Adcox, et al., Formation of dense partonic matter in relativistic nucleus-nucleus collisions at RHIC: experimental evaluation by the PHENIX collaboration, Nucl. Phys. A 757 (2005) 184–283, arXiv:nucl-ex/0410003 [nucl-ex].

[6] BRAHMS Collaboration, I. Arsene, et al., Quark gluon plasma and color glass condensate at RHIC? The Perspective from the BRAHMS experiment, Nucl. Phys. A 757 (2005) 1–27, arXiv:nucl-ex/0410020 [nucl-ex].

[7] PHOBOS Collaboration, B.B. Back, et al., The PHOBOS perspective on discoveries at RHIC, Nucl. Phys. A 757 (2005) 28–101, arXiv:nucl-ex/0410022 [nucl-ex].

[8] M. Gyulassy, L. McLerran, New forms of QCD matter discovered at RHIC, Nucl. Phys. A 750 (2005) 30–63, arXiv:nucl-th/0405013 [nucl-th].

[9] E. Shuryak, Physics of strongly coupled quark-gluon plasma, Prog. Part. Nucl. Phys. 62 (2009) 48–101, arXiv:0807.3033 [hep-ph].

[10] STAR Collaboration, M.M. Aggarwal, et al., K^{*0} production in Cu+Cu and Au+Au collisions at $\sqrt{s_{NN}}$ = 62.4 GeV and 200 GeV, Phys. Rev. C 84 (2011) 034909, arXiv:1006.1961 [nucl-ex].

[11] STAR Collaboration, J. Adams, et al., $K^{*}(892)^{0}$ resonance production in Au+Au and p+p collisions at $\sqrt{s_{NN}}$ = 200 GeV at STAR, Phys. Rev. C 71 (2005) 064902, arXiv:nucl-ex/0412019 [nucl-ex].

[12] STAR Collaboration, B.I. Abelev, et al., Strange baryon resonance production in $\sqrt{s_{NN}}$ = 200-GeV p+p and Au+Au collisions, Phys. Rev. Lett. 97 (2006) 132301, arXiv:nucl-ex/0604019 [nucl-ex].

[13] ALICE Collaboration, S. Acharya, et al., Suppression of $\Lambda(1520)$ resonance production in central Pb–Pb collisions at $\sqrt{s_{NN}}$ = 2.76 TeV, Phys. Rev. C 99 (2019) 024905, arXiv:1805.04361 [nucl-ex].

[14] ALICE Collaboration, B. Abelev, et al., $K^{*}(892)^{0}$ and $\phi(1020)$ production in Pb–Pb collisions at $\sqrt{s_{NN}}$ = 2.76 TeV, Phys. Rev. C 91 (2015) 024609, arXiv:1404.0495 [nucl-ex].

[15] ALICE Collaboration, S. Acharya, et al., Production of the $\rho(770)^{0}$ meson in pp and Pb–Pb collisions at $\sqrt{s_{NN}}$ = 2.76 TeV, Phys. Rev. C 99 (6) (2019) 064901, arXiv:1805.04365 [nucl-ex].

[16] STAR Collaboration, B.I. Abelev, et al., Energy and system size dependence of ϕ meson production in Cu+Cu and Au+Au collisions, Phys. Lett. B 673 (2009) 183–191, arXiv:0810.4979 [nucl-ex].

[17] ALICE Collaboration, J. Adam, et al., Production of K* (892)^{0} and ϕ (1020) in p–Pb collisions at $\sqrt{s_{NN}}$ = 5.02 TeV, Eur. Phys. J. C 76 (5) (2016) 245, arXiv:1601.07868 [nucl-ex].

[18] ALICE Collaboration, B. Abelev, et al., Production of $K^{*}(892)^{0}$ and $\phi(1020)$ in pp collisions at $\sqrt{s}$ = 7 TeV, Eur. Phys. J. C 72 (2012) 2183, arXiv:1208.5717 [hep-ex].

[19] STAR Collaboration, B.I. Abelev, et al., Hadronic resonance production in d+Au collisions at $\sqrt{s_{NN}}$ = 200-GeV at RHIC, Phys. Rev. C 78 (2008) 044906, arXiv:0801.0450 [nucl-ex].

[20] Particle Data Group Collaboration, M. Tanabashi, et al., Review of particle physics, Phys. Rev. D 98 (3) (2018) 030001.

[21] G.E. Brown, M. Rho, Scaling effective Lagrangians in a dense medium, Phys. Rev. Lett. 66 (1991) 2720–2723.

[22] M. Bleicher, J. Aichelin, Strange resonance production: probing chemical and thermal freezeout in relativistic heavy ion collisions, Phys. Lett. B 530 (2002) 81–87, arXiv:hep-ph/0201123 [hep-ph].

[23] G. Torrieri, J. Rafelski, Strange hadron resonances as a signature of freezeout dynamics, Phys. Lett. B 509 (2001) 239–245, arXiv:hep-ph/0103149 [hep-ph].

[24] S.C. Johnson, B.V. Jacak, A. Drees, Rescattering of vector meson daughters in high-energy heavy ion collisions, Eur. Phys. J. C 18 (2001) 645–649, arXiv:nucl-th/9909075 [nucl-th].

[25] C. Markert, R. Bellwied, I. Vitev, Formation and decay of hadronic resonances in the QGP, Phys. Lett. B 669 (2008) 92–97, arXiv:0807.1509 [nucl-th].

[26] A. Ilner, J. Blair, D. Cabrera, C. Markert, E. Bratkovskaya, Probing the hot and dense nuclear matter with K^{*}, $\bar{K}^{*}$ vector mesons, Phys. Rev. C 99 (2) (2019) 024914, arXiv:1707.00060 [hep-ph].

[27] V.M. Shapoval, P. Braun-Munzinger, Yu.M. Sinyukov, $K^*(892)$ and $\phi(1020)$ production and their decay into the hadronic medium at the Large Hadron Collider, Nucl. Phys. A 968 (2017) 391–402, arXiv:1707.06753 [hep-ph].

[28] R. Rapp, E.V. Shuryak, Resolving the anti-baryon production puzzle in high-energy heavy ion collisions, Phys. Rev. Lett. 86 (2001) 2980–2983, arXiv:hep-ph/0008326 [hep-ph].

[29] C. Song, V. Koch, Chemical relaxation time of pions in hot hadronic matter, Phys. Rev. C 55 (1997) 3026–3037, arXiv:nucl-th/9611034 [nucl-th].

[30] J. Rafelski, J. Letessier, G. Torrieri, Strange hadrons and their resonances: a diagnostic tool of QGP freezeout dynamics, Phys. Rev. C 64 (2001) 054907, arXiv:nucl-th/0104042 [nucl-th];
J. Rafelski, J. Letessier, G. Torrieri, Phys. Rev. C 65 (2002) 069902 (Erratum).

[31] S. Singha, B. Mohanty, Z.-W. Lin, Studying re-scattering effect in heavy-ion collision through K* production, Int. J. Mod. Phys. E 24 (05) (2015) 1550041, arXiv:1505.02342 [nucl-ex].

[32] A.G. Knospe, C. Markert, K. Werner, J. Steinheimer, M. Bleicher, Hadronic resonance production and interaction in partonic and hadronic matter in the EPOS3 model with and without the hadronic afterburner UrQMD, Phys. Rev. C 93 (1) (2016) 014911, arXiv:1509.07895 [nucl-th].

[33] A. Andronic, P. Braun-Munzinger, J. Stachel, Thermal hadron production in relativistic nuclear collisions: the Hadron mass spectrum, the horn, and the QCD phase transition, Phys. Lett. B 673 (2009) 142–145, arXiv:0812.1186 [nucl-th];
A. Andronic, P. Braun-Munzinger, J. Stachel, Phys. Lett. B 678 (2009) 516 (Erratum).

[34] A. Andronic, P. Braun-Munzinger, K. Redlich, J. Stachel, Decoding the phase structure of QCD via particle production at high energy, Nature 561 (7723) (2018) 321–330, arXiv:1710.09425 [nucl-th].

[35] J. Cleymans, K. Redlich, Chemical and thermal freezeout parameters from 1 AGeV to 200 AGeV, Phys. Rev. C 60 (1999) 054908, arXiv:nucl-th/9903063 [nucl-th].

[36] S. Chatterjee, S. Das, L. Kumar, D. Mishra, B. Mohanty, R. Sahoo, N. Sharma, Freeze-out parameters in heavy-ion collisions at AGS, SPS, RHIC, and LHC energies, Adv. High Energy Phys. 2015 (2015) 349013.

[37] W. Broniowski, W. Florkowski, B. Hiller, Thermal analysis of production of resonances in relativistic heavy ion collisions, Phys. Rev. C 68 (2003) 034911, arXiv:nucl-th/0306034 [nucl-th].

[38] R. Rapp, π^+-π^- emission in high-energy nuclear collisions, Nucl. Phys. A 725 (2003) 254–268, arXiv:hep-ph/0305011 [hep-ph].

[39] S.D. Protopopescu, M. Alston-Garnjost, A. Barbaro-Galtieri, S.M. Flatte, J.H. Friedman, T.A. Lasinski, G.R. Lynch, M.S. Rabin, F.T. Solmitz, $\pi\pi$ partial wave analysis from reactions $\pi^+ p \rightarrow \pi^+ \pi^- \Delta^{++}$ and $\pi^+ p \rightarrow K^+ K^- \Delta^{++}$ at 7.1-GeV/c, Phys. Rev. D 7 (1973) 1279.

[40] M.J. Matison, A. Barbaro-Galtieri, M. Alston-Garnjost, S.M. Flatte, J.H. Friedman, G.R. Lynch, M.S. Rabin, F. Solmitz, Study of $K^+ \pi^-$ scattering in the reaction $K^+ p \rightarrow K^+ \pi^- \Delta^{++}$ at 12-GeV/c, Phys. Rev. D 9 (1974) 1872.

[41] M. Bleicher, et al., Relativistic hadron hadron collisions in the ultrarelativistic quantum molecular dynamics model, J. Phys. G 25 (1999) 1859–1896, arXiv:hep-ph/9909407 [hep-ph].

[42] ALICE Collaboration, J. Adam, et al., $K^*(892)^0$ and $\phi(1020)$ meson production at high transverse momentum in pp and Pb–Pb collisions at $\sqrt{s_{NN}}$ = 2.76 TeV, Phys. Rev. C 95 (6) (2017) 064606, arXiv:1702.00555 [nucl-ex].

[43] ALICE Collaboration, P. Cortese, et al., ALICE: physics performance report, vol. II, J. Phys. G 32 (2006) 1295–2040.

[44] ALICE Collaboration, K. Aamodt, et al., The ALICE experiment at the CERN LHC, J. Instrum. 3 (2008) S08002.

[45] ALICE Collaboration, B. Abelev, et al., Performance of the ALICE experiment at the CERN LHC, Int. J. Mod. Phys. A 29 (2014) 1430044, arXiv:1402.4476 [nucl-ex].

[46] ALICE Collaboration, J. Adam, et al., Centrality dependence of the charged-particle multiplicity density at midrapidity in Pb–Pb collisions at $\sqrt{s_{NN}}$ = 5.02 TeV, Phys. Rev. Lett. 116 (22) (2016) 222302, arXiv:1512.06104 [nucl-ex].

[47] ALICE Collaboration, K. Aamodt, et al., Centrality dependence of the charged-particle multiplicity density at mid-rapidity in Pb–Pb collisions at $\sqrt{s_{NN}}$ = 2.76 TeV, Phys. Rev. Lett. 106 (2011) 032301, arXiv:1012.1657 [nucl-ex].

[48] ALICE Collaboration, J. Adam, et al., Determination of the event collision time with the ALICE detector at the LHC, Eur. Phys. J. Plus 132 (2) (2017) 99, arXiv:1610.03055 [physics.ins-det].

[49] ALICE Collaboration, P. Cortese, et al., ALICE technical design report on forward detectors: FMD, T0 and V0, CERN-LHCC-2004-025, 2004.

[50] ALICE Collaboration, E. Abbas, et al., Performance of the ALICE VZERO system, J. Instrum. 8 (2013) P10016, arXiv:1306.3130 [nucl-ex].

[51] ALICE Collaboration, S. Acharya, et al., Production of charged pions, kaons and (anti-)protons in Pb-Pb and inelastic pp collisions at $\sqrt{s_{NN}}$ = 5.02 TeV, arXiv:1910.07678 [nucl-ex].

[52] P.Z. Skands, Tuning Monte Carlo generators: the Perugia tunes, Phys. Rev. D 82 (2010) 074018, arXiv:1005.3457 [hep-ph].

[53] P. Skands, S. Carrazza, J. Rojo, Tuning PYTHIA 8.1: the Monash 2013 tune, Eur. Phys. J. C 74 (8) (2014) 3024, arXiv:1404.5630 [hep-ph].

[54] X.-N. Wang, M. Gyulassy, HIJING: a Monte Carlo model for multiple jet production in p p, p A and A A collisions, Phys. Rev. D 44 (1991) 3501–3516.

[55] R. Brun, F. Bruyant, F. Carminati, S. Giani, M. Maire, A. McPherson, G. Patrick, L. Urban, GEANT: Detector Description and Simulation Tool, CERN Program Library. Long Writeup W5013, 1993, http://cds.cern.ch/record/1082634.

[56] C. Loizides, J. Kamin, D. d'Enterria, Improved Monte Carlo Glauber predictions at present and future nuclear colliders, Phys. Rev. C 97 (5) (2018) 054910, arXiv:1710.07098;
C. Loizides, J. Kamin, D. d'Enterria, Phys. Rev. C 99 (1) (2019) 019901 (Erratum).

[57] ALICE Collaboration, B. Abelev, et al., Production of charged pions, kaons and protons at large transverse momenta in pp and Pb–Pb collisions at $\sqrt{s_{NN}}$ = 2.76 TeV, Phys. Lett. B 736 (2014) 196–207, arXiv:1401.1250 [nucl-ex].

[58] C. Tsallis, Possible generalization of Boltzmann-Gibbs statistics, J. Stat. Phys. 52 (1988) 479–487.

[59] STAR Collaboration, B.I. Abelev, et al., Strange particle production in p+p collisions at $\sqrt{s_{NN}}$ = 200 GeV, Phys. Rev. C 75 (2007) 064901, arXiv:nucl-ex/0607033 [nucl-ex].

[60] E. Schnedermann, J. Sollfrank, U.W. Heinz, Thermal phenomenology of hadrons from 200A GeV S+S collisions, Phys. Rev. C 48 (1993) 2462–2475, arXiv:nucl-th/9307020 [nucl-th].

[61] ALICE Collaboration, K. Aamodt, et al., Two-pion Bose-Einstein correlations in central Pb–Pb collisions at $\sqrt{s_{NN}}$ = 2.76 TeV, Phys. Lett. B 696 (2011) 328–337, arXiv:1012.4035 [nucl-ex].

[62] M.A. Lisa, S. Pratt, R. Soltz, U. Wiedemann, Femtoscopy in relativistic heavy ion collisions, Annu. Rev. Nucl. Part. Sci. 55 (2005) 357–402, arXiv:nucl-ex/0505014 [nucl-ex].

[63] S.A. Bass, A. Dumitru, M. Bleicher, L. Bravina, E. Zabrodin, H. Stoecker, W. Greiner, Hadronic freezeout following a first order hadronization phase transition in ultrarelativistic heavy ion collisions, Phys. Rev. C 60 (1999) 021902, arXiv:nucl-th/9902062 [nucl-th].

[64] J. Stachel, A. Andronic, P. Braun-Munzinger, K. Redlich, Confronting LHC data with the statistical hadronization model, J. Phys. Conf. Ser. 509 (2014) 012019, arXiv:1311.4662 [nucl-th].

[65] C. Shen, U. Heinz, P. Huovinen, H. Song, Radial and elliptic flow in Pb+Pb collisions at the Large Hadron Collider from viscous hydrodynamics, Phys. Rev. C 84 (2011) 044903, arXiv:1105.3226 [nucl-th].

[66] V. Minissale, F. Scardina, V. Greco, Hadrons from coalescence plus fragmentation in AA collisions at energies available at the BNL Relativistic Heavy Ion Collider to the CERN Large Hadron Collider, Phys. Rev. C 92 (5) (2015) 054904, arXiv:1502.06213 [nucl-th].

ALICE Collaboration

S. Acharya [141], D. Adamová [94], A. Adler [74], J. Adolfsson [80], M.M. Aggarwal [99], G. Aglieri Rinella [33], M. Agnello [30], N. Agrawal [10,53], Z. Ahammed [141], S. Ahmad [16], S.U. Ahn [76], A. Akindinov [91], M. Al-Turany [106], S.N. Alam [141], D.S.D. Albuquerque [122], D. Aleksandrov [87], B. Alessandro [58], H.M. Alfanda [6], R. Alfaro Molina [71], B. Ali [16], Y. Ali [14], A. Alici [10,26,53], A. Alkin [2], J. Alme [21], T. Alt [68], L. Altenkamper [21], I. Altsybeev [112], M.N. Anaam [6], C. Andrei [47], D. Andreou [33], H.A. Andrews [110], A. Andronic [144], M. Angeletti [33], V. Anguelov [103], C. Anson [15], T. Antičić [107], F. Antinori [56], P. Antonioli [53], R. Anwar [125], N. Apadula [79], L. Aphecetche [114], H. Appelshäuser [68], S. Arcelli [26], R. Arnaldi [58], M. Arratia [79], I.C. Arsene [20], M. Arslandok [103], A. Augustinus [33], R. Averbeck [106], S. Aziz [61], M.D. Azmi [16], A. Badalà [55], Y.W. Baek [40], S. Bagnasco [58], X. Bai [106], R. Bailhache [68], R. Bala [100], A. Baldisseri [137], M. Ball [42],

S. Balouza [104], R. Barbera [27], L. Barioglio [25], G.G. Barnaföldi [145], L.S. Barnby [93], V. Barret [134], P. Bartalini [6], K. Barth [33], E. Bartsch [68], F. Baruffaldi [28], N. Bastid [134], S. Basu [143], G. Batigne [114], B. Batyunya [75], D. Bauri [48], J.L. Bazo Alba [111], I.G. Bearden [88], C. Bedda [63], N.K. Behera [60], I. Belikov [136], A.D.C. Bell Hechavarria [144], F. Bellini [33], R. Bellwied [125], V. Belyaev [92], G. Bencedi [145], S. Beole [25], A. Bercuci [47], Y. Berdnikov [97], D. Berenyi [145], R.A. Bertens [130], D. Berzano [58], M.G. Besoiu [67], L. Betev [33], A. Bhasin [100], I.R. Bhat [100], M.A. Bhat [3], H. Bhatt [48], B. Bhattacharjee [41], A. Bianchi [25], L. Bianchi [25], N. Bianchi [51], J. Bielčík [36], J. Bielčíková [94], A. Bilandzic [104,117], G. Biro [145], R. Biswas [3], S. Biswas [3], J.T. Blair [119], D. Blau [87], C. Blume [68], G. Boca [139], F. Bock [33,95], A. Bogdanov [92], S. Boi [23], L. Boldizsár [145], A. Bolozdynya [92], M. Bombara [37], G. Bonomi [140], H. Borel [137], A. Borissov [92,144], H. Bossi [146], E. Botta [25], L. Bratrud [68], P. Braun-Munzinger [106], M. Bregant [121], M. Broz [36], E.J. Brucken [43], E. Bruna [58], G.E. Bruno [105], M.D. Buckland [127], D. Budnikov [108], H. Buesching [68], S. Bufalino [30], O. Bugnon [114], P. Buhler [113], P. Buncic [33], Z. Buthelezi [72,131], J.B. Butt [14], J.T. Buxton [96], S.A. Bysiak [118], D. Caffarri [89], A. Caliva [106], E. Calvo Villar [111], R.S. Camacho [44], P. Camerini [24], A.A. Capon [113], F. Carnesecchi [10,26], R. Caron [137], J. Castillo Castellanos [137], A.J. Castro [130], E.A.R. Casula [54], F. Catalano [30], C. Ceballos Sanchez [52], P. Chakraborty [48], S. Chandra [141], W. Chang [6], S. Chapeland [33], M. Chartier [127], S. Chattopadhyay [141], S. Chattopadhyay [109], A. Chauvin [23], C. Cheshkov [135], B. Cheynis [135], V. Chibante Barroso [33], D.D. Chinellato [122], S. Cho [60], P. Chochula [33], T. Chowdhury [134], P. Christakoglou [89], C.H. Christensen [88], P. Christiansen [80], T. Chujo [133], C. Cicalo [54], L. Cifarelli [10,26], F. Cindolo [53], J. Cleymans [124], F. Colamaria [52], D. Colella [52], A. Collu [79], M. Colocci [26], M. Concas [58,ii], G. Conesa Balbastre [78], Z. Conesa del Valle [61], G. Contin [24,127], J.G. Contreras [36], T.M. Cormier [95], Y. Corrales Morales [25], P. Cortese [31], M.R. Cosentino [123], F. Costa [33], S. Costanza [139], P. Crochet [134], E. Cuautle [69], P. Cui [6], L. Cunqueiro [95], D. Dabrowski [142], T. Dahms [104,117], A. Dainese [56], F.P.A. Damas [114,137], M.C. Danisch [103], A. Danu [67], D. Das [109], I. Das [109], P. Das [85], P. Das [3], S. Das [3], A. Dash [85], S. Dash [48], S. De [85], A. De Caro [29], G. de Cataldo [52], J. de Cuveland [38], A. De Falco [23], D. De Gruttola [10], N. De Marco [58], S. De Pasquale [29], S. Deb [49], B. Debjani [3], H.F. Degenhardt [121], K.R. Deja [142], A. Deloff [84], S. Delsanto [25,131], D. Devetak [106], P. Dhankher [48], D. Di Bari [32], A. Di Mauro [33], R.A. Diaz [8], T. Dietel [124], P. Dillenseger [68], Y. Ding [6], R. Divià [33], D.U. Dixit [19], Ø. Djuvsland [21], U. Dmitrieva [62], A. Dobrin [33,67], B. Dönigus [68], O. Dordic [20], A.K. Dubey [141], A. Dubla [106], S. Dudi [99], M. Dukhishyam [85], P. Dupieux [134], R.J. Ehlers [146], V.N. Eikeland [21], D. Elia [52], H. Engel [74], E. Epple [146], B. Erazmus [114], F. Erhardt [98], A. Erokhin [112], M.R. Ersdal [21], B. Espagnon [61], G. Eulisse [33], D. Evans [110], S. Evdokimov [90], L. Fabbietti [104,117], M. Faggin [28], J. Faivre [78], F. Fan [6], A. Fantoni [51], M. Fasel [95], P. Fecchio [30], A. Feliciello [58], G. Feofilov [112], A. Fernández Téllez [44], A. Ferrero [137], A. Ferretti [25], A. Festanti [33], V.J.G. Feuillard [103], J. Figiel [118], S. Filchagin [108], D. Finogeev [62], F.M. Fionda [21], G. Fiorenza [52], F. Flor [125], S. Foertsch [72], P. Foka [106], S. Fokin [87], E. Fragiacomo [59], U. Frankenfeld [106], U. Fuchs [33], C. Furget [78], A. Furs [62], M. Fusco Girard [29], J.J. Gaardhøje [88], M. Gagliardi [25], A.M. Gago [111], A. Gal [136], C.D. Galvan [120], P. Ganoti [83], C. Garabatos [106], E. Garcia-Solis [11], K. Garg [27], C. Gargiulo [33], A. Garibli [86], K. Garner [144], P. Gasik [104,117], E.F. Gauger [119], M.B. Gay Ducati [70], M. Germain [114], J. Ghosh [109], P. Ghosh [141], S.K. Ghosh [3], P. Gianotti [51], P. Giubellino [58,106], P. Giubilato [28], P. Glässel [103], D.M. Gómez Coral [71], A. Gomez Ramirez [74], V. Gonzalez [106], P. González-Zamora [44], S. Gorbunov [38], L. Görlich [118], S. Gotovac [34], V. Grabski [71], L.K. Graczykowski [142], K.L. Graham [110], L. Greiner [79], A. Grelli [63], C. Grigoras [33], V. Grigoriev [92], A. Grigoryan [1], S. Grigoryan [75], O.S. Groettvik [21], F. Grosa [30], J.F. Grosse-Oetringhaus [33], R. Grosso [106], R. Guernane [78], M. Guittiere [114], K. Gulbrandsen [88], T. Gunji [132], A. Gupta [100], R. Gupta [100], I.B. Guzman [44], R. Haake [146], M.K. Habib [106], C. Hadjidakis [61], H. Hamagaki [81], G. Hamar [145], M. Hamid [6], R. Hannigan [119], M.R. Haque [63,85], A. Harlenderova [106], J.W. Harris [146], A. Harton [11], J.A. Hasenbichler [33], H. Hassan [95], D. Hatzifotiadou [10,53], P. Hauer [42], S. Hayashi [132], S.T. Heckel [68,104], E. Hellbär [68], H. Helstrup [35], A. Herghelegiu [47], T. Herman [36], E.G. Hernandez [44], G. Herrera Corral [9], F. Herrmann [144], K.F. Hetland [35], T.E. Hilden [43], H. Hillemanns [33], C. Hills [127], B. Hippolyte [136], B. Hohlweger [104], D. Horak [36], A. Hornung [68], S. Hornung [106], R. Hosokawa [15,133], P. Hristov [33], C. Huang [61], C. Hughes [130], P. Huhn [68], T.J. Humanic [96], H. Hushnud [109], L.A. Husova [144], N. Hussain [41], S.A. Hussain [14], D. Hutter [38], J.P. Iddon [33,127], R. Ilkaev [108], M. Inaba [133], G.M. Innocenti [33], M. Ippolitov [87], A. Isakov [94], M.S. Islam [109], M. Ivanov [106], V. Ivanov [97], V. Izucheev [90], B. Jacak [79], N. Jacazio [53], P.M. Jacobs [79], S. Jadlovska [116], J. Jadlovsky [116], S. Jaelani [63], C. Jahnke [121],

M.J. Jakubowska [142], M.A. Janik [142], T. Janson [74], C. Jena [85], M. Jercic [98], O. Jevons [110], M. Jin [125], F. Jonas [95,144], P.G. Jones [110], J. Jung [68], M. Jung [68], A. Jusko [110], P. Kalinak [64], A. Kalweit [33], V. Kaplin [92], S. Kar [6], A. Karasu Uysal [77], O. Karavichev [62], T. Karavicheva [62], P. Karczmarczyk [33], E. Karpechev [62], A. Kazantsev [87], U. Kebschull [74], R. Keidel [46], M. Keil [33], B. Ketzer [42], Z. Khabanova [89], A.M. Khan [6], S. Khan [16], S.A. Khan [141], A. Khanzadeev [97], Y. Kharlov [90], A. Khatun [16], A. Khuntia [118], B. Kileng [35], B. Kim [60], B. Kim [133], D. Kim [147], D.J. Kim [126], E.J. Kim [73], H. Kim [17,147], J. Kim [147], J.S. Kim [40], J. Kim [103], J. Kim [147], J. Kim [73], M. Kim [103], S. Kim [18], T. Kim [147], T. Kim [147], S. Kirsch [38,68], I. Kisel [38], S. Kiselev [91], A. Kisiel [142], J.L. Klay [5], C. Klein [68], J. Klein [58], S. Klein [79], C. Klein-Bösing [144], M. Kleiner [68], A. Kluge [33], M.L. Knichel [33], A.G. Knospe [125], C. Kobdaj [115], M.K. Köhler [103], T. Kollegger [106], A. Kondratyev [75], N. Kondratyeva [92], E. Kondratyuk [90], J. Konig [68], P.J. Konopka [33], L. Koska [116], O. Kovalenko [84], V. Kovalenko [112], M. Kowalski [118], I. Králik [64], A. Kravčáková [37], L. Kreis [106], M. Krivda [64,110], F. Krizek [94], K. Krizkova Gajdosova [36], M. Krüger [68], E. Kryshen [97], M. Krzewicki [38], A.M. Kubera [96], V. Kučera [60], C. Kuhn [136], P.G. Kuijer [89], L. Kumar [99], S. Kumar [48], S. Kundu [85], P. Kurashvili [84], A. Kurepin [62], A.B. Kurepin [62], A. Kuryakin [108], S. Kushpil [94], J. Kvapil [110], M.J. Kweon [60], J.Y. Kwon [60], Y. Kwon [147], S.L. La Pointe [38], P. La Rocca [27], Y.S. Lai [79], R. Langoy [129], K. Lapidus [33], A. Lardeux [20], P. Larionov [51], E. Laudi [33], R. Lavicka [36], T. Lazareva [112], R. Lea [24], L. Leardini [103], J. Lee [133], S. Lee [147], F. Lehas [89], S. Lehner [113], J. Lehrbach [38], R.C. Lemmon [93], I. León Monzón [120], E.D. Lesser [19], M. Lettrich [33], P. Lévai [145], X. Li [12], X.L. Li [6], J. Lien [129], R. Lietava [110], B. Lim [17], V. Lindenstruth [38], S.W. Lindsay [127], C. Lippmann [106], M.A. Lisa [96], V. Litichevskyi [43], A. Liu [19], S. Liu [96], W.J. Llope [143], I.M. Lofnes [21], V. Loginov [92], C. Loizides [95], P. Loncar [34], X. Lopez [134], E. López Torres [8], J.R. Luhder [144], M. Lunardon [28], G. Luparello [59], Y. Ma [39], A. Maevskaya [62], M. Mager [33], S.M. Mahmood [20], T. Mahmoud [42], A. Maire [136], R.D. Majka [146], M. Malaev [97], Q.W. Malik [20], L. Malinina [75,iii], D. Mal'Kevich [91], P. Malzacher [106], G. Mandaglio [55], V. Manko [87], F. Manso [134], V. Manzari [52], Y. Mao [6], M. Marchisone [135], J. Mareš [66], G.V. Margagliotti [24], A. Margotti [53], J. Margutti [63], A. Marín [106], C. Markert [119], M. Marquard [68], N.A. Martin [103], P. Martinengo [33], J.L. Martinez [125], M.I. Martínez [44], G. Martínez García [114], M. Martinez Pedreira [33], S. Masciocchi [106], M. Masera [25], A. Masoni [54], L. Massacrier [61], E. Masson [114], A. Mastroserio [52,138], A.M. Mathis [104,117], O. Matonoha [80], P.F.T. Matuoka [121], A. Matyja [118], C. Mayer [118], M. Mazzilli [52], M.A. Mazzoni [57], A.F. Mechler [68], F. Meddi [22], Y. Melikyan [62,92], A. Menchaca-Rocha [71], C. Mengke [6], E. Meninno [29,113], M. Meres [13], S. Mhlanga [124], Y. Miake [133], L. Micheletti [25], D.L. Mihaylov [104], K. Mikhaylov [75,91], A. Mischke [63,i], A.N. Mishra [69], D. Miśkowiec [106], A. Modak [3], N. Mohammadi [33], A.P. Mohanty [63], B. Mohanty [85], M. Mohisin Khan [16,iv], C. Mordasini [104], D.A. Moreira De Godoy [144], L.A.P. Moreno [44], I. Morozov [62], A. Morsch [33], T. Mrnjavac [33], V. Muccifora [51], E. Mudnic [34], D. Mühlheim [144], S. Muhuri [141], J.D. Mulligan [79], M.G. Munhoz [121], R.H. Munzer [68], H. Murakami [132], S. Murray [124], L. Musa [33], J. Musinsky [64], C.J. Myers [125], J.W. Myrcha [142], B. Naik [48], R. Nair [84], B.K. Nandi [48], R. Nania [10,53], E. Nappi [52], M.U. Naru [14], A.F. Nassirpour [80], C. Nattrass [130], R. Nayak [48], T.K. Nayak [85], S. Nazarenko [108], A. Neagu [20], R.A. Negrao De Oliveira [68], L. Nellen [69], S.V. Nesbo [35], G. Neskovic [38], D. Nesterov [112], L.T. Neumann [142], B.S. Nielsen [88], S. Nikolaev [87], S. Nikulin [87], V. Nikulin [97], F. Noferini [10,53], P. Nomokonov [75], J. Norman [78,127], N. Novitzky [133], P. Nowakowski [142], A. Nyanin [87], J. Nystrand [21], M. Ogino [81], A. Ohlson [80,103], J. Oleniacz [142], A.C. Oliveira Da Silva [121,130], M.H. Oliver [146], C. Oppedisano [58], R. Orava [43], A. Ortiz Velasquez [69], A. Oskarsson [80], J. Otwinowski [118], K. Oyama [81], Y. Pachmayer [103], V. Pacik [88], D. Pagano [140], G. Paić [69], J. Pan [143], A.K. Pandey [48], S. Panebianco [137], P. Pareek [49,141], J. Park [60], J.E. Parkkila [126], S. Parmar [99], S.P. Pathak [125], R.N. Patra [141], B. Paul [23,58], H. Pei [6], T. Peitzmann [63], X. Peng [6], L.G. Pereira [70], H. Pereira Da Costa [137], D. Peresunko [87], G.M. Perez [8], E. Perez Lezama [68], V. Peskov [68], Y. Pestov [4], V. Petráček [36], M. Petrovici [47], R.P. Pezzi [70], S. Piano [59], M. Pikna [13], P. Pillot [114], O. Pinazza [33,53], L. Pinsky [125], C. Pinto [27], S. Pisano [10,51], D. Pistone [55], M. Płoskoń [79], M. Planinic [98], F. Pliquett [68], J. Pluta [142], S. Pochybova [145,i], M.G. Poghosyan [95], B. Polichtchouk [90], N. Poljak [98], A. Pop [47], H. Poppenborg [144], S. Porteboeuf-Houssais [134], V. Pozdniakov [75], S.K. Prasad [3], R. Preghenella [53], F. Prino [58], C.A. Pruneau [143], I. Pshenichnov [62], M. Puccio [25,33], J. Putschke [143], R.E. Quishpe [125], S. Ragoni [110], S. Raha [3], S. Rajput [100], J. Rak [126], A. Rakotozafindrabe [137], L. Ramello [31], F. Rami [136], R. Raniwala [101], S. Raniwala [101], S.S. Räsänen [43], R. Rath [49], V. Ratza [42], I. Ravasenga [30,89], K.F. Read [95,130], K. Redlich [84,v], A. Rehman [21], P. Reichelt [68], F. Reidt [33], X. Ren [6], R. Renfordt [68], Z. Rescakova [37], J.-P. Revol [10], K. Reygers [103], V. Riabov [97], T. Richert [80,88], M. Richter [20],

P. Riedler [33], W. Riegler [33], F. Riggi [27], C. Ristea [67], S.P. Rode [49], M. Rodríguez Cahuantzi [44], K. Røed [20], R. Rogalev [90], E. Rogochaya [75], D. Rohr [33], D. Röhrich [21], P.S. Rokita [142], F. Ronchetti [51], E.D. Rosas [69], K. Roslon [142], A. Rossi [28,56], A. Rotondi [139], A. Roy [49], P. Roy [109], O.V. Rueda [80], R. Rui [24], B. Rumyantsev [75], A. Rustamov [86], E. Ryabinkin [87], Y. Ryabov [97], A. Rybicki [118], H. Rytkonen [126], O.A.M. Saarimaki [43], S. Sadhu [141], S. Sadovsky [90], K. Šafařík [36], S.K. Saha [141], B. Sahoo [48], P. Sahoo [48,49], R. Sahoo [49], S. Sahoo [65], P.K. Sahu [65], J. Saini [141], S. Sakai [133], S. Sambyal [100], V. Samsonov [92,97], D. Sarkar [143], N. Sarkar [141], P. Sarma [41], V.M. Sarti [104], M.H.P. Sas [63], E. Scapparone [53], B. Schaefer [95], J. Schambach [119], H.S. Scheid [68], C. Schiaua [47], R. Schicker [103], A. Schmah [103], C. Schmidt [106], H.R. Schmidt [102], M.O. Schmidt [103], M. Schmidt [102], N.V. Schmidt [68,95], A.R. Schmier [130], J. Schukraft [88], Y. Schutz [33,136], K. Schwarz [106], K. Schweda [106], G. Scioli [26], E. Scomparin [58], M. Šefčík [37], J.E. Seger [15], Y. Sekiguchi [132], D. Sekihata [132], I. Selyuzhenkov [92,106], S. Senyukov [136], D. Serebryakov [62], E. Serradilla [71], A. Sevcenco [67], A. Shabanov [62], A. Shabetai [114], R. Shahoyan [33], W. Shaikh [109], A. Shangaraev [90], A. Sharma [99], A. Sharma [100], H. Sharma [118], M. Sharma [100], N. Sharma [99], A.I. Sheikh [141], K. Shigaki [45], M. Shimomura [82], S. Shirinkin [91], Q. Shou [39], Y. Sibiriak [87], S. Siddhanta [54], T. Siemiarczuk [84], D. Silvermyr [80], G. Simatovic [89], G. Simonetti [33,104], R. Singh [85], R. Singh [100], R. Singh [49], V.K. Singh [141], V. Singhal [141], T. Sinha [109], B. Sitar [13], M. Sitta [31], T.B. Skaali [20], M. Slupecki [126], N. Smirnov [146], R.J.M. Snellings [63], T.W. Snellman [43,126], C. Soncco [111], J. Song [60,125], A. Songmoolnak [115], F. Soramel [28], S. Sorensen [130], I. Sputowska [118], J. Stachel [103], I. Stan [67], P. Stankus [95], P.J. Steffanic [130], E. Stenlund [80], D. Stocco [114], M.M. Storetvedt [35], L.D. Stritto [29], A.A.P. Suaide [121], T. Sugitate [45], C. Suire [61], M. Suleymanov [14], M. Suljic [33], R. Sultanov [91], M. Šumbera [94], S. Sumowidagdo [50], S. Swain [65], A. Szabo [13], I. Szarka [13], U. Tabassam [14], G. Taillepied [134], J. Takahashi [122], G.J. Tambave [21], S. Tang [6,134], M. Tarhini [114], M.G. Tarzila [47], A. Tauro [33], G. Tejeda Muñoz [44], A. Telesca [33], C. Terrevoli [125], D. Thakur [49], S. Thakur [141], D. Thomas [119], F. Thoresen [88], R. Tieulent [135], A. Tikhonov [62], A.R. Timmins [125], A. Toia [68], N. Topilskaya [62], M. Toppi [51], F. Torales-Acosta [19], S.R. Torres [9,120], A. Trifiro [55], S. Tripathy [49], T. Tripathy [48], S. Trogolo [28], G. Trombetta [32], L. Tropp [37], V. Trubnikov [2], W.H. Trzaska [126], T.P. Trzcinski [142], B.A. Trzeciak [63], T. Tsuji [132], A. Tumkin [108], R. Turrisi [56], T.S. Tveter [20], K. Ullaland [21], E.N. Umaka [125], A. Uras [135], G.L. Usai [23], A. Utrobicic [98], M. Vala [37], N. Valle [139], S. Vallero [58], N. van der Kolk [63], L.V.R. van Doremalen [63], M. van Leeuwen [63], P. Vande Vyvre [33], D. Varga [145], Z. Varga [145], M. Varga-Kofarago [145], A. Vargas [44], M. Vasileiou [83], A. Vasiliev [87], O. Vázquez Doce [104,117], V. Vechernin [112], A.M. Veen [63], E. Vercellin [25], S. Vergara Limón [44], L. Vermunt [63], R. Vernet [7], R. Vértesi [145], L. Vickovic [34], Z. Vilakazi [131], O. Villalobos Baillie [110], A. Villatoro Tello [44], G. Vino [52], A. Vinogradov [87], T. Virgili [29], V. Vislavicius [88], A. Vodopyanov [75], B. Volkel [33], M.A. Völkl [102], K. Voloshin [91], S.A. Voloshin [143], G. Volpe [32], B. von Haller [33], I. Vorobyev [104], D. Voscek [116], J. Vrláková [37], B. Wagner [21], M. Weber [113], S.G. Weber [144], A. Wegrzynek [33], D.F. Weiser [103], S.C. Wenzel [33], J.P. Wessels [144], J. Wiechula [68], J. Wikne [20], G. Wilk [84], J. Wilkinson [10,53], G.A. Willems [33], E. Willsher [110], B. Windelband [103], M. Winn [137], W.E. Witt [130], Y. Wu [128], R. Xu [6], S. Yalcin [77], K. Yamakawa [45], S. Yang [21], S. Yano [137], Z. Yin [6], H. Yokoyama [63], I.-K. Yoo [17], J.H. Yoon [60], S. Yuan [21], A. Yuncu [103], V. Yurchenko [2], V. Zaccolo [24], A. Zaman [14], C. Zampolli [33], H.J.C. Zanoli [63], N. Zardoshti [33], A. Zarochentsev [112], P. Závada [66], N. Zaviyalov [108], H. Zbroszczyk [142], M. Zhalov [97], S. Zhang [39], X. Zhang [6], Z. Zhang [6], V. Zherebchevskii [112], D. Zhou [6], Y. Zhou [88], Z. Zhou [21], J. Zhu [6,106], Y. Zhu [6], A. Zichichi [10,26], M.B. Zimmermann [33], G. Zinovjev [2], N. Zurlo [140]

[1] *A.I. Alikhanyan National Science Laboratory (Yerevan Physics Institute) Foundation, Yerevan, Armenia*
[2] *Bogolyubov Institute for Theoretical Physics, National Academy of Sciences of Ukraine, Kiev, Ukraine*
[3] *Bose Institute, Department of Physics and Centre for Astroparticle Physics and Space Science (CAPSS), Kolkata, India*
[4] *Budker Institute for Nuclear Physics, Novosibirsk, Russia*
[5] *California Polytechnic State University, San Luis Obispo, CA, United States*
[6] *Central China Normal University, Wuhan, China*
[7] *Centre de Calcul de l'IN2P3, Villeurbanne, Lyon, France*
[8] *Centro de Aplicaciones Tecnológicas y Desarrollo Nuclear (CEADEN), Havana, Cuba*
[9] *Centro de Investigación y de Estudios Avanzados (CINVESTAV), Mexico City and Mérida, Mexico*
[10] *Centro Fermi – Museo Storico della Fisica e Centro Studi e Ricerche "Enrico Fermi", Rome, Italy*
[11] *Chicago State University, Chicago, IL, United States*
[12] *China Institute of Atomic Energy, Beijing, China*
[13] *Comenius University Bratislava, Faculty of Mathematics, Physics and Informatics, Bratislava, Slovakia*
[14] *COMSATS University Islamabad, Islamabad, Pakistan*
[15] *Creighton University, Omaha, NE, United States*
[16] *Department of Physics, Aligarh Muslim University, Aligarh, India*

[17] *Department of Physics, Pusan National University, Pusan, Republic of Korea*
[18] *Department of Physics, Sejong University, Seoul, Republic of Korea*
[19] *Department of Physics, University of California, Berkeley, CA, United States*
[20] *Department of Physics, University of Oslo, Oslo, Norway*
[21] *Department of Physics and Technology, University of Bergen, Bergen, Norway*
[22] *Dipartimento di Fisica dell'Università 'La Sapienza' and Sezione INFN, Rome, Italy*
[23] *Dipartimento di Fisica dell'Università and Sezione INFN, Cagliari, Italy*
[24] *Dipartimento di Fisica dell'Università and Sezione INFN, Trieste, Italy*
[25] *Dipartimento di Fisica dell'Università and Sezione INFN, Turin, Italy*
[26] *Dipartimento di Fisica e Astronomia dell'Università and Sezione INFN, Bologna, Italy*
[27] *Dipartimento di Fisica e Astronomia dell'Università and Sezione INFN, Catania, Italy*
[28] *Dipartimento di Fisica e Astronomia dell'Università and Sezione INFN, Padova, Italy*
[29] *Dipartimento di Fisica 'E.R. Caianiello' dell'Università and Gruppo Collegato INFN, Salerno, Italy*
[30] *Dipartimento DISAT del Politecnico and Sezione INFN, Turin, Italy*
[31] *Dipartimento di Scienze e Innovazione Tecnologica dell'Università del Piemonte Orientale and INFN Sezione di Torino, Alessandria, Italy*
[32] *Dipartimento Interateneo di Fisica 'M. Merlin' and Sezione INFN, Bari, Italy*
[33] *European Organization for Nuclear Research (CERN), Geneva, Switzerland*
[34] *Faculty of Electrical Engineering, Mechanical Engineering and Naval Architecture, University of Split, Split, Croatia*
[35] *Faculty of Engineering and Science, Western Norway University of Applied Sciences, Bergen, Norway*
[36] *Faculty of Nuclear Sciences and Physical Engineering, Czech Technical University in Prague, Prague, Czech Republic*
[37] *Faculty of Science, P.J. Šafárik University, Košice, Slovakia*
[38] *Frankfurt Institute for Advanced Studies, Johann Wolfgang Goethe-Universität Frankfurt, Frankfurt, Germany*
[39] *Fudan University, Shanghai, China*
[40] *Gangneung-Wonju National University, Gangneung, Republic of Korea*
[41] *Gauhati University, Department of Physics, Guwahati, India*
[42] *Helmholtz-Institut für Strahlen- und Kernphysik, Rheinische Friedrich-Wilhelms-Universität Bonn, Bonn, Germany*
[43] *Helsinki Institute of Physics (HIP), Helsinki, Finland*
[44] *High Energy Physics Group, Universidad Autónoma de Puebla, Puebla, Mexico*
[45] *Hiroshima University, Hiroshima, Japan*
[46] *Hochschule Worms, Zentrum für Technologietransfer und Telekommunikation (ZTT), Worms, Germany*
[47] *Horia Hulubei National Institute of Physics and Nuclear Engineering, Bucharest, Romania*
[48] *Indian Institute of Technology Bombay (IIT), Mumbai, India*
[49] *Indian Institute of Technology Indore, Indore, India*
[50] *Indonesian Institute of Sciences, Jakarta, Indonesia*
[51] *INFN, Laboratori Nazionali di Frascati, Frascati, Italy*
[52] *INFN, Sezione di Bari, Bari, Italy*
[53] *INFN, Sezione di Bologna, Bologna, Italy*
[54] *INFN, Sezione di Cagliari, Cagliari, Italy*
[55] *INFN, Sezione di Catania, Catania, Italy*
[56] *INFN, Sezione di Padova, Padova, Italy*
[57] *INFN, Sezione di Roma, Rome, Italy*
[58] *INFN, Sezione di Torino, Turin, Italy*
[59] *INFN, Sezione di Trieste, Trieste, Italy*
[60] *Inha University, Incheon, Republic of Korea*
[61] *Institut de Physique Nucléaire d'Orsay (IPNO), Institut National de Physique Nucléaire et de Physique des Particules (IN2P3/CNRS), Université de Paris-Sud, Université Paris-Saclay, Orsay, France*
[62] *Institute for Nuclear Research, Academy of Sciences, Moscow, Russia*
[63] *Institute for Subatomic Physics, Utrecht University/Nikhef, Utrecht, Netherlands*
[64] *Institute of Experimental Physics, Slovak Academy of Sciences, Košice, Slovakia*
[65] *Institute of Physics, Homi Bhabha National Institute, Bhubaneswar, India*
[66] *Institute of Physics of the Czech Academy of Sciences, Prague, Czech Republic*
[67] *Institute of Space Science (ISS), Bucharest, Romania*
[68] *Institut für Kernphysik, Johann Wolfgang Goethe-Universität Frankfurt, Frankfurt, Germany*
[69] *Instituto de Ciencias Nucleares, Universidad Nacional Autónoma de México, Mexico City, Mexico*
[70] *Instituto de Física, Universidade Federal do Rio Grande do Sul (UFRGS), Porto Alegre, Brazil*
[71] *Instituto de Física, Universidad Nacional Autónoma de México, Mexico City, Mexico*
[72] *iThemba LABS, National Research Foundation, Somerset West, South Africa*
[73] *Jeonbuk National University, Jeonju, Republic of Korea*
[74] *Johann-Wolfgang-Goethe Universität Frankfurt Institut für Informatik, Fachbereich Informatik und Mathematik, Frankfurt, Germany*
[75] *Joint Institute for Nuclear Research (JINR), Dubna, Russia*
[76] *Korea Institute of Science and Technology Information, Daejeon, Republic of Korea*
[77] *KTO Karatay University, Konya, Turkey*
[78] *Laboratoire de Physique Subatomique et de Cosmologie, Université Grenoble-Alpes, CNRS-IN2P3, Grenoble, France*
[79] *Lawrence Berkeley National Laboratory, Berkeley, CA, United States*
[80] *Lund University Department of Physics, Division of Particle Physics, Lund, Sweden*
[81] *Nagasaki Institute of Applied Science, Nagasaki, Japan*
[82] *Nara Women's University (NWU), Nara, Japan*
[83] *National and Kapodistrian University of Athens, School of Science, Department of Physics, Athens, Greece*
[84] *National Centre for Nuclear Research, Warsaw, Poland*
[85] *National Institute of Science Education and Research, Homi Bhabha National Institute, Jatni, India*
[86] *National Nuclear Research Center, Baku, Azerbaijan*
[87] *National Research Centre Kurchatov Institute, Moscow, Russia*
[88] *Niels Bohr Institute, University of Copenhagen, Copenhagen, Denmark*
[89] *Nikhef, National institute for subatomic physics, Amsterdam, Netherlands*
[90] *NRC Kurchatov Institute IHEP, Protvino, Russia*
[91] *NRC "Kurchatov Institute" – ITEP, Moscow, Russia*
[92] *NRNU Moscow Engineering Physics Institute, Moscow, Russia*
[93] *Nuclear Physics Group, STFC Daresbury Laboratory, Daresbury, United Kingdom*
[94] *Nuclear Physics Institute of the Czech Academy of Sciences, Řež u Prahy, Czech Republic*

[95] Oak Ridge National Laboratory, Oak Ridge, TN, United States
[96] Ohio State University, Columbus, OH, United States
[97] Petersburg Nuclear Physics Institute, Gatchina, Russia
[98] Physics department, Faculty of science, University of Zagreb, Zagreb, Croatia
[99] Physics Department, Panjab University, Chandigarh, India
[100] Physics Department, University of Jammu, Jammu, India
[101] Physics Department, University of Rajasthan, Jaipur, India
[102] Physikalisches Institut, Eberhard-Karls-Universität Tübingen, Tübingen, Germany
[103] Physikalisches Institut, Ruprecht-Karls-Universität Heidelberg, Heidelberg, Germany
[104] Physik Department, Technische Universität München, Munich, Germany
[105] Politecnico di Bari, Bari, Italy
[106] Research Division and ExtreMe Matter Institute EMMI, GSI Helmholtzzentrum für Schwerionenforschung GmbH, Darmstadt, Germany
[107] Rudjer Bošković Institute, Zagreb, Croatia
[108] Russian Federal Nuclear Center (VNIIEF), Sarov, Russia
[109] Saha Institute of Nuclear Physics, Homi Bhabha National Institute, Kolkata, India
[110] School of Physics and Astronomy, University of Birmingham, Birmingham, United Kingdom
[111] Sección Física, Departamento de Ciencias, Pontificia Universidad Católica del Perú, Lima, Peru
[112] St. Petersburg State University, St. Petersburg, Russia
[113] Stefan Meyer Institut für Subatomare Physik (SMI), Vienna, Austria
[114] SUBATECH, IMT Atlantique, Université de Nantes, CNRS-IN2P3, Nantes, France
[115] Suranaree University of Technology, Nakhon Ratchasima, Thailand
[116] Technical University of Košice, Košice, Slovakia
[117] Technische Universität München, Excellence Cluster 'Universe', Munich, Germany
[118] The Henryk Niewodniczanski Institute of Nuclear Physics, Polish Academy of Sciences, Cracow, Poland
[119] The University of Texas at Austin, Austin, TX, United States
[120] Universidad Autónoma de Sinaloa, Culiacán, Mexico
[121] Universidade de São Paulo (USP), São Paulo, Brazil
[122] Universidade Estadual de Campinas (UNICAMP), Campinas, Brazil
[123] Universidade Federal do ABC, Santo Andre, Brazil
[124] University of Cape Town, Cape Town, South Africa
[125] University of Houston, Houston, TX, United States
[126] University of Jyväskylä, Jyväskylä, Finland
[127] University of Liverpool, Liverpool, United Kingdom
[128] University of Science and Techonology of China, Hefei, China
[129] University of South-Eastern Norway, Tonsberg, Norway
[130] University of Tennessee, Knoxville, TN, United States
[131] University of the Witwatersrand, Johannesburg, South Africa
[132] University of Tokyo, Tokyo, Japan
[133] University of Tsukuba, Tsukuba, Japan
[134] Université Clermont Auvergne, CNRS/IN2P3, LPC, Clermont-Ferrand, France
[135] Université de Lyon, Université Lyon 1, CNRS/IN2P3, IPN-Lyon, Villeurbanne, Lyon, France
[136] Université de Strasbourg, CNRS, IPHC UMR 7178, F-67000 Strasbourg, France, Strasbourg, France
[137] Université Paris-Saclay Centre d'Etudes de Saclay (CEA), IRFU, Départment de Physique Nucléaire (DPhN), Saclay, France
[138] Università degli Studi di Foggia, Foggia, Italy
[139] Università degli Studi di Pavia, Pavia, Italy
[140] Università di Brescia, Brescia, Italy
[141] Variable Energy Cyclotron Centre, Homi Bhabha National Institute, Kolkata, India
[142] Warsaw University of Technology, Warsaw, Poland
[143] Wayne State University, Detroit, MI, United States
[144] Westfälische Wilhelms-Universität Münster, Institut für Kernphysik, Münster, Germany
[145] Wigner Research Centre for Physics, Budapest, Hungary
[146] Yale University, New Haven, CT, United States
[147] Yonsei University, Seoul, Republic of Korea

[i] Deceased.
[ii] Dipartimento DET del Politecnico di Torino, Turin, Italy.
[iii] M.V. Lomonosov Moscow State University, D.V. Skobeltsyn Institute of Nuclear, Physics, Moscow, Russia.
[iv] Department of Applied Physics, Aligarh Muslim University, Aligarh, India.
[v] Institute of Theoretical Physics, University of Wroclaw, Poland.